

9 Studies of acid-base status and regulation

Hans-Otto Pörtner¹, Ulf Bickmeyer¹, Markus Bleich², Christian Bock¹, Colin Brownlee³, Frank Melzner⁴, Basile Michaelidis⁵, Franz-Josef Sartoris¹ and Daniela Storch¹

¹Alfred Wegener Institute for Polar and Marine Research, Germany

²Institute of Physiology, Christian-Albrechts-University, Germany

³Marine Biological Association, UK

⁴Leibniz-Institute of Marine Sciences, IFM-GEOMAR, Germany

⁵School of Biology, Aristotle University of Thessaloniki, Greece

9.1 Introduction

The emerging threat of ocean acidification for marine life has re-emphasised the crucial importance of acid-base status and regulation in whole organism functional maintenance and enantiostasis. pH values in different body compartments are widely accepted to play a key role in the maintenance of physiological function or their limitation under functional or environmental stress. pH affects protein function in metabolism and oxygen transport. Also, acid-base and metabolic regulation are interdependent processes in a way that changes in pH affect metabolic rate, the mode of catabolism and energetic parameters (Pörtner, 1989).

However, acid-base regulation not only means adjustment or maintenance of pH which, in turn, is perceived as the key acid-base parameter influencing regulatory processes. Under certain conditions and with the help of the respective membrane carriers (see below), priority may rather be given to the regulation of the concentrations of bases (carbonate, bicarbonate) or acid (carbonic acid, which is proportional to CO₂ partial pressure) in body fluids. pH then becomes a dependent variable. Also, in some studies, it is not pH which is of interest but rather the activity of protons a_{H^+} , $\text{pH} = -\log_{10}(a_{\text{H}^+})$, for example when protons contribute to some biochemical reactions or affect protein carriers in a concentration dependent manner (see equation 9.1, as an example). In general, biochemical studies of acid-base regulation usually focus on intracellular pH as a key parameter related to protein function, whereas physiological, cellular and especially whole animal studies have always considered the close interrelationships between pH and the CO₂/bicarbonate system in intra- and extracellular fluids (Siggaard-Andersen, 1974). Furthermore, the involvement of CO₂ and bicarbonate as substrates or products in enzymatic reactions (Pörtner, 1989; Walsh & Milligan, 1989; Hardewig *et al.*, 1994) led to the development of physiological concepts of acid-base regulation in metabolic biochemistry.

Acid-base regulation is an energy dependent process since some of the acid-base equivalents are transported by H⁺-ATPases or by processes exploiting the Na⁺-gradient established by Na⁺/K⁺-ATPase, for example Na⁺/H⁺ or sodium dependent Cl⁻/HCO₃⁻ exchangers. Species are capable of modulating the cost of acid-base regulation. Conversely, the rate and efficiency of acid-base regulation are influenced by the value of pH that is reached or that can be maintained by the ion exchange mechanisms involved in regulation (e.g. Reipschläger & Pörtner, 1996; Pörtner *et al.*, 2000). In addition, the significance of metabolism for acid-base regulation has been discussed, from disturbances of acid-base status to metabolic contributions to acid-base regulation, with some ongoing debate (Hochachka & Mommsen, 1983; Pörtner, 1987a, 1995; Atkinson & Bourke, 1995; Robergs *et al.*, 2004, Prakash *et al.*, 2008). Quantifying acid-base parameters *per se* remains insufficient to gain a deeper understanding of the ecological role of acid-base physiology. This requires addressing the effects of acid-base variables on metabolic processes and species performances (e.g. exercise, growth, shell structure and calcification, reproduction) and fitness. Such relationships have rarely been investigated. Most importantly, changes in acid-base variables in the organism should be considered as mediators of effects and not just as effects *per se* (Pörtner *et al.*, 2005).

9.2 Fundamentals of acid-base regulation

9.2.1 A comprehensive set of acid-base parameters in whole organism research

Acid-base regulation occurs at systemic (extracellular), cellular and subcellular levels. For unicellular marine organisms, seawater is the extracellular fluid. In animals, the composition of seawater has been modified into the ones of haemolymph, coelomic fluid, interstitial fluid and blood. For ocean acidification research, acid-base parameters should ideally be determined in relevant compartments of whole organisms and in conditions as close as possible to their natural situation (for example animals dwelling in burrows), or in animals during and after exercise. As a trade-off, analyses may need to be carried out in isolated organs or cellular preparations of organisms acclimated to CO₂ levels according to ocean acidification scenarios. Acclimation would ideally be long term (weeks or months), possibly followed by analyses of short-term modifications (seconds to minutes), for example during study of muscular activity under elevated CO₂ levels. During studies in live animals, development of a quantitative picture of acid-base status should include parallel analyses of acid-base parameters in both intra- and extracellular fluids as well as in ambient water. This includes measurement of pH, P_{CO₂} and the concentrations of bicarbonate and carbonate in the compartments of interest. Furthermore, the buffer value of non-bicarbonate buffers resisting such changes by proton binding or release must also be known. Such quantification of acid-base variables will reveal the net movement of acid-base equivalents between compartments, across membranes or epithelia (cf. Heisler, 1989). In the context of ocean acidification and ocean warming it needs to be considered that regulated set points of acid-base regulation are not invariant, but are dynamic depending on the physiological condition of the organism and are, moreover, influenced by ambient parameters such as temperature and CO₂.

Reeves (1972, 1985) introduced the imidazole α -stat hypothesis stating that poikilotherms regulate pH such that the degree of protonation (α) of imidazole groups is maintained despite changes in body temperature. The importance of this concept is emphasised by the observation that the average pK of histidyl residues exposed to the solvent falls in the vicinity of pH_i values of typical cells (Somero, 1986). Thus, relatively small changes in pK_i could produce significant changes in protein ionisation. The α -stat concept implies that changes in pH fully or partly offset temperature-induced changes in protein ionisation thereby maintaining relative constancy of protein structure and function. Since the pK of imidazole groups may (on average) change by $-0.018^\circ\text{C}^{-1}$, a shift in intra- and extracellular pH with body temperature by $\Delta\text{pH}/\Delta T \sim -0.018^\circ\text{C}^{-1}$ enables α to remain constant. α -stat pH regulation is also beneficial for the energy status. A pH rise with falling temperature ensures that the ATP free energy is maintained at a high level (Pörtner *et al.*, 1998). Cameron (1989) proposed the “Z-stat” model which emphasises that protein net charge Z is maintained rather than α in diverse histidine groups. Z-stat is a consequence of the maintenance of mean α for any protein mixture. $\Delta\text{pK } ^\circ\text{C}^{-1}$ depends upon local charge configurations in the environment of the imidazole group as well as on ionic strength and, therefore, varies between -0.016 and $-0.024^\circ\text{C}^{-1}$ for histidine and free imidazole compounds and ranges between -0.001 and $-0.051^\circ\text{C}^{-1}$ for histidine residues in proteins (Heisler, 1986). Overall, pH changes with temperature in marine ectotherms support the concept but can deviate from the theoretical value of $-0.018^\circ\text{C}^{-1}$ depending on the physiological situation of the organism (cf. Pörtner *et al.*, 1998).

9.2.2 Physicochemistry of body fluids: pH bicarbonate analysis

It is crucial that analyses of compartmental physicochemistry quantify the acid-base parameters, which are affecting the components and thermodynamics of biological processes in a concentration-dependent manner. These parameters usually include the free concentrations or activities of solutes such as CO₂, protons, bicarbonate and/or carbonate ions. The disturbance of body and cell compartments by elevated CO₂ levels also depends on the concentration and characteristics of buffers (e.g. phosphates, imidazole groups in proteins and amino acids), summarised as the non-bicarbonate buffer value β_{NB} (mmol H⁺ l⁻¹ pH⁻¹). pH in body fluids has traditionally been determined on the NBS pH scale using IUPAC high precision buffers (e.g. Buck *et*

al., 2002). For pH analyses in seawater, ocean chemists have developed specific procedures and buffers in line with different pH scales; the free, total and seawater pH scales (Zeebe & Wolf-Gladrow, 2001; chapter 1 of this guide). The issue of how ocean physicochemistry impacts on marine organisms requires bringing the oceanographic and physiological approaches together. The inclusion of sulfate protonation equilibria into the total pH scale and of both sulfate and fluoride protonation into the seawater pH scale enhances the precision in quantifying changes in ocean physicochemistry. However, this inclusion means that the total and seawater scales do not represent the pH effective on biological material. Dissociation equilibria depend on ionic strength and on proton activity (cf. Pörtner, 1990). When studying effects of seawater pH on function in marine invertebrates, the free pH scale (which excludes protons bound to sulfate and fluoride) thus appears most suitable. The dissociation equilibria of sulfate and fluoride, which are included in the total and seawater pH scales, respectively, are pH-dependent variables and do not interfere or interact with the pH-dependent protonation of biological material. Since seawater buffers are set to calibrate electrodes on total scale, free pH must be determined from total pH by calculation.

The ionic strength of extracellular invertebrate body fluids is similar to the ionic strength of seawater. The use of the free pH scale in both seawater and invertebrate extracellular fluid would support comparing the pH values in both fluids and accurately quantifying the pH gradients between them. The calibration on total scale involves the use of appropriate buffers at seawater ionic strength. This would reduce the errors introduced by shifting liquid junction potentials of pH electrodes when calibrating and measuring solutions of largely different ionic strengths (Dickson *et al.*, 2007). Marine organisms also enter estuaries or brackish waters with variable osmolarities. Precise measurements of pH in their body fluids benefit from the use of buffers with the corresponding ionic composition and strength. Recipes and equations for the preparation of such synthetic seawater buffer solutions of different salinities (using Tris/HCl and 2-aminopyridine/HCl) are available in Dickson *et al.* (2007) (Chapter SOP 6a).

However, the use of the NBS pH scale in both seawater and extracellular fluid would still quantify pH gradients correctly, although absolute pH values differ somewhat from those on the free scale. In general, the use of the NBS pH scale for body fluids allows the use of well-established physiological concepts and methodologies (see below). In both invertebrates and fish tissues, or in all body fluids of marine teleost fishes, the NBS scale appears the most appropriate at present, due to ionic concentrations and osmolarities similarly low as in mammalian tissues and body fluids. The same likely applies to marine invertebrate osmoconformers living in brackish water. In any case, measuring relative pH changes over time within one compartment requires using the same calibration method throughout. In the future, a continuum of pH calibrations at various ionic strengths would help to bring ocean chemists and biologists together to address the acid-base physiology of marine organisms in response to ocean acidification. In the following, all pH values refer to the NBS scale. Measurements in the extracellular fluids of marine invertebrates or seawater involve the use of pH electrodes equilibrated in seawater prior to calibration and also prior to the actual analyses in body fluids.

The pH/bicarbonate diagram, also called Davenport-diagram (Figure 9.1) quantifies respiratory (via changes in P_{CO_2}) and non-respiratory processes contributing to changes in the acid-base status. Non-respiratory changes in a compartment comprise the influence of metabolic pathways and the net exchange of acid or base equivalents across epithelia or membranes. Also included in the non-respiratory processes are any changes in the protonation of proteins associated with the binding or release of ligands (e.g. oxygen binding or release from haemoglobin or haemocyanin, cf. Pörtner, 1990b). The pH/bicarbonate diagram illustrates the relationships between pH, bicarbonate concentrations and P_{CO_2} as they result from the Henderson-Hasselbalch-equation of the CO_2 /bicarbonate system (Figure 9.2). The analysis of the acid-base status quantifies the changes in pH, bicarbonate concentration, P_{CO_2} , and non-bicarbonate buffer value β_{NB} in the various compartments. The total (tot.) change in pH comprises a respiratory (resp.) and a non-respiratory (non-resp.) component. The respiratory component of the pH change is derived from the change in P_{CO_2} along the buffer line, in accordance with the titration of the non-bicarbonate buffer mix by CO_2 . This process leads to changes in pH and in bicarbonate levels in opposite direction (pH falls and the bicarbonate level rises). Accordingly, respiratory proton quantities are determined

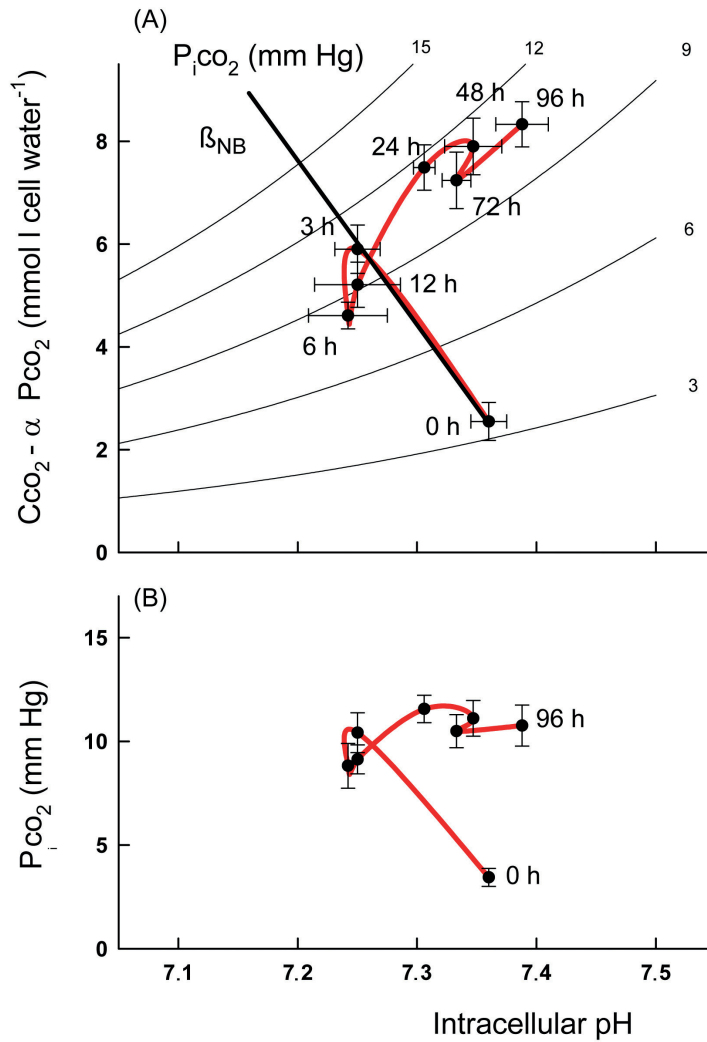


Figure 9.1 pH bicarbonate diagram (A) depicting the interrelated changes of intracellular acid-base variables pH (pH_i), bicarbonate and P_iCO₂ (P_iCO₂) over time and in relation to the non-bicarbonate buffer (β_{NB}) line. Initial changes in pH_i are driven by the accumulation of CO₂ which leads to a rise in P_iCO₂ (B), titrates non-bicarbonate buffers and is therefore paralleled by an accumulation of bicarbonate (A). Transmembrane ion exchange and metabolic processes interfere after 3 h and, after an initial base loss, lead to continued net bicarbonate accumulation while the respiratory acidosis persists with more or less constant P_iCO₂ levels (based on data from Pörtner *et al.*, 1998).

during pH/bicarbonate analysis as the bicarbonate increment along the buffer line β_{NB}, starting from a control point specified by a combination of pH, bicarbonate and P_iCO₂ values (equation 9.1).

$$\Delta\text{pH}_{\text{resp.}} \times -|\beta_{\text{NB}}| = \Delta[\text{HCO}_3^-]_{\text{resp.}} = -\Delta\text{H}^+_{\text{resp.}} \quad (9.1)$$

In contrast, non-respiratory changes in the acid-base status cause a unidirectional change in both pH and bicarbonate levels (Figure 9.1B). It follows one of the P_iCO₂ isopleths starting from a control point in the graph defined by pH, bicarbonate and P_iCO₂. The respective proton quantities causing such changes are calculated from the changes in pH and bicarbonate concentration along the P_iCO₂ isopleth considering the non-bicarbonate buffer value (equation 9.2).

$$\Delta\text{H}^+_{\text{non-resp.}} = \left(\Delta\text{pH}_{\text{tot.}} \times -|\beta_{\text{NB}}| \right) - \Delta[\text{HCO}_3^-]_{\text{tot.}} \quad (9.2)$$

Usually, a change in acid-base status is caused by a mix of respiratory and non-respiratory disturbances. Equation 9.2 is still valid when the change in pH and bicarbonate concentration are affected by respiratory processes, indicated by a change in P_{CO_2} . The dissolution of carbonates is also taken into account through its effects on pH and on the concentration of bicarbonate. Since a respiratory change in pH is associated with a change in bicarbonate levels in the opposite direction (equation 9.1), respiratory changes always balance to 0 in equation 9.2.

9.3 Measurement of pH, total CO_2 and non-bicarbonate buffer values

For optimal cellular function, intracellular pH (pH_i) is tightly controlled particularly within the cytosol, through the effect of mechanisms such as intracellular buffering and membrane transport (including ATP-driven H^+ pumps, exchangers and ion channels). H^+ gradients maintained between the intracellular and extracellular spaces are used for membrane transport of substrates and ions, e.g. dipeptides (Daniel & Kottra, 2004) and Na^+ (Biemesderfer *et al.*, 1993). Understanding the mechanisms that regulate intracellular pH is a prerequisite for estimating the effects of long-term pH perturbations on pH-dependent intracellular processes. For a meaningful interpretation of the impact of ocean acidification on marine organisms (Pörtner *et al.*, 2005) measurements of intracellular pH require the knowledge of extracellular pH (pH_e). The maintenance of extracellular pH is a highly dynamic process, which feeds back on the regulation of pH_i (Pörtner *et al.*, 2000). Thus, a comparison of intracellular pH between systems is meaningless without knowledge of pH_e (Gillies *et al.*, 1994).

$$\begin{array}{c}
 \overbrace{CO_2 + H_2O \leftrightarrow H_2CO_3}^A \leftrightarrow H^+ + HCO_3^- \leftrightarrow 2H^+ + CO_3^{2-} + Na^+ \leftrightarrow 2H^+ + NaCO_3^- \\
 \underbrace{H^+ + HCO_3^-}_{B} \quad \underbrace{2H^+ + CO_3^{2-} + Na^+}_{D} \\
 pH = pK_1''' + \log_{10} \frac{[HCO_3^-]'}{\alpha_{CO_2} \times P_{CO_2}} \rightarrow [HCO_3^-]' = C_{CO_2} - \alpha_{CO_2} \times P_{CO_2} \\
 \alpha_{CO_2} = 0.1008 - 29.80 \times 10^{-3}[M] + (1.218 \times 10^{-3}[M] - 3.639 \times 10^{-3})t \\
 \quad - (19.57 \times 10^{-6}[M] - 69.59 \times 10^{-6})t^2 \\
 \quad + (71.71 \times 10^9[M] - 559.6 \times 10^{-9})t^3 \text{ (mmol l}^{-1} \cdot \text{mm Hg}^{-1}) \\
 pK_{1app}''' = \underbrace{6.583 - 13.41 \times 10^{-3}t + 228.2 \times 10^{-6}t^2 - 1.516 \times 10^{-6}t^3 - 0.341I^{0.323}}_A \\
 \quad - \log_{10} \left\{ \underbrace{1 + 0.00039[Pr]}_B + \underbrace{10^{pH - 10.64 + 0.011t + 0.737I^{0.323}}}_C \right. \\
 \quad \left. \times \underbrace{\left(1 + 10^{1.92 - 0.01t - 0.737I^{0.323} + \log_{10}[Na^+]} + (-0.494I + 0.651)(1 + 0.0065[Pr]) \right)}_D \right\} \rightarrow [HCO_3^-]'
 \end{array}$$

Figure 9.2 Calculation of constants used to determine the physicochemical variables in body fluid compartments of animals (after Heisler, 1984, 1986). pK''' is the apparent dissociation constant of the CO_2 /apparent bicarbonate ' $[HCO_3^-]'$ ' system. α_{CO_2} is the physical solubility of CO_2 . C_{CO_2} is the total CO_2 content of body fluids. Note that these equations comprise adjustments to variable ion and protein concentrations and ionic strength, and are applicable to seawater (cf. Pörtner *et al.*, 1998). Terms A-D refer to the respective reaction equilibria considered in the calculation of pK''' . M is the molarity of dissolved species (volume of protein and salt subtracted), t is the temperature ($^{\circ}C$, range 0 - 40 $^{\circ}C$) and I is the ionic strength of non-protein ions; $I = 0.5 \sum ([x]Z^2)$, where $[x]$ is the concentration in mol l^{-1} and Z is the number of charges of the respective ion. $[Na^+]$ is the sodium concentration (mol l^{-1}) and $[Pr]$ is the protein concentration (g l^{-1}).

A variety of techniques have been used to measure pH in body fluids and tissues. They include glass electrodes, combination glass electrodes, ion-sensitive microelectrodes, glass microelectrodes, fluorescent dyes, pH-optodes, ISFET (Ion-Sensitive Field Effect Transistor) sensors and NMR (Nuclear Magnetic Resonance) spectroscopy. All methods have their pros and cons and often have overlapping areas of application. They are confronted with the need to analyse acid-base variables under undisturbed conditions, i.e. the result of the measurement should not be influenced by the measurement procedure itself. These issues are dealt with below.

The calibration of pH electrodes or optodes requires buffers that must be designed to match the ionic composition and strength of the respective compartment (see above). Ionic strength is similar in seawater and in the extracellular fluid of marine invertebrates, but is lower in the body fluids of fish, and in the intracellular compartments of all organisms. A shift in ion composition occurs from predominantly Na⁺ in extracellular to predominantly K⁺ in intracellular fluids.

9.3.1 Capillary pH electrodes, microelectrodes, pH optodes

Measurements of extracellular pH with capillary or micro-glass electrodes and pH optodes require sample volumes of 0.2 to 100 µl, or the implantation of the electrode or optode inside the body compartment. The optode can be used for online pH recordings by implanting it like a cannula. In this case no blood needs to be withdrawn.

Ideally, the pH of extracellular fluid (pH_e) is measured using Radiometer glass capillary pH electrodes (G299A) or equivalent design with separate glass and reference electrodes for highest precision. Unfortunately, the capillary electrodes are no longer commercially available. Most pH microelectrodes are combination electrodes, which combine both an H⁺ ion sensitive glass electrode, and a reference electrode into one housing. The change in potential ΔE (V) across the ion sensitive glass with a change in pH is usually given by a simplified Nernst equation (the factor 0.0591 is valid at 25°C):

$$\Delta E = 0.0591 \times \Delta \text{pH} \quad (9.3)$$

Accordingly, calibration is required prior to use. Since the relationship between the electrode potential and pH of the solution is linear over a wide range of pHs it is sufficient to calibrate the electrode using two buffer solutions of known pH. Miniaturisation of the electrode is limited by the combination of two electrodes in one body. The tip diameter of commercially available micro pH electrodes ranges from 1 to 3 mm with an immersion depth of 1 to 3 mm resulting in a sample volume of about 10 to 100 µl. However, both the accuracy and the precision of microelectrodes decrease with decreasing size and range between 0.01 to 0.02 pH units (Kratz, 1950).

Most of the new optical pH sensors (pH optodes, e.g. pH HPS-OIW, PreSens, Regensburg, Germany) are fluorescence-based and measure the pH dependent luminescence decay time. No reference electrode is needed which allows minimisation of the optode tip down to 20 µm, enabling pH measurement in the sub-microliter range. Optodes are useful in the physiologically relevant pH range of pH 6 to 9. The response time ranges between 15 and 30 s at temperatures above 15°C and the accuracy and precision are better than 0.02 to 0.05 pH units in body fluids and reach up to about 0.01 pH units in seawater. The pH response is not linear and calibration may thus require more than two buffers, unless buffers are chosen close to the actual pH values of the sample. The sensitivity to ionic strength (salinity) is higher than in glass electrodes and fluorescent molecules in the sample may also interfere with the measurement (Wolfbeis, 1991; Kosch *et al.*, 1998; Liebsch *et al.*, 2001). Nonetheless, promising results have been obtained for measurements of intracellular pH (T. Hirse & H.-O. Pörtner, unpubl.), as well as for pH determinations in cephalopod blood and egg perivitelline fluid (Melzner, 2005; Gutowska & Melzner, 2009; Gutowska *et al.*, 2009).

The electrode or optode can be implanted into the wall of a syringe so that it is immersed into the sample when the syringe is filled. However, the sample volume required may become substantial (200 µl). Recently, a syringe setup with a combined oxygen and pH optode has been used for repeated sampling of haemolymph from a cephalopod during hypercapnic exposure (Gutowska *et al.*, 2009). Owing to the high sensitivity of the system to variable ionic strength, calibration was performed using plasma from the experimental animals

following termination of the experiment. The plasma was equilibrated under different CO₂-air mixtures using a tonometer in order to reach different pH values.

During alternative measurement scenarios the blood sample is transferred to a small Eppendorf cap in which pH is measured. However, this procedure comes with the inherent risk of gas exchange between the sample and the air, and an associated drift in pH readings. Insertion into a glass capillary with an outer diameter only slightly larger than the electrode tip alleviates this problem and minimises air contact. The small tip diameter of a pH optode also allows insertion (under optical control with a binocular) through the needle into a syringe or into a glass capillary filled with body fluid (Thatje *et al.*, 2003; Welker *et al.*, 2007).

Strengths and weaknesses

The newest generation of pH glass electrodes is the result of almost 100 years of development and experience (Haber & Klemensiewicz, 1909). Special electrodes are available for a great variety of applications (e.g. high protein content or low salinity), but the availability of some types (e.g. capillary pH electrodes) is limited, as instrumentation developed for manual blood gas analyses in human blood samples has gone out of production. pH microelectrodes should be used whenever the sample volume is sufficient. In small samples and in high magnetic fields (e.g. NMR) pH-sensitive optodes are a suitable alternative. In addition, optodes are implantable (as established for oxygen optodes, cf. Frederich & Pörtner, 2000; Sartoris *et al.*, 2003; Lannig *et al.*, 2004; Melzner *et al.*, 2006a; Metzger *et al.*, 2007) allowing to measure blood/haemolymph Po₂ or pH online in fish and invertebrates. pH optodes need to be cross-calibrated with pH glass electrodes in the same media to detect any discrepancies depending on ionic strength.

Calibration procedures should use precision NBS buffers, or buffers allowing to determine free pH at adequate ionic strength and to cover the range of expected pH values. A two-point calibration is sufficient for electrodes. Ideally, buffers should have the same ionic strength as the sample, especially when using optodes. However, commercially available buffers usually do not fulfil this criterion. Seawater buffers can be made according to the recipes given by Dickson *et al.* (2007). Electrodes, which have a low cross sensitivity to ionic strength (salinity), should be equilibrated in a solution with the same ionic strength and composition as the sample prior to calibration and measurements. This procedure enhances accuracy and minimises memory effects and drift. For optodes, which have a high sensitivity to ionic strength and a non-linear pH response, calibration buffers must be adjusted to the appropriate ionic strength or be custom-made. The error needs to be quantified by cross calibration with glass electrodes. Coloured buffer solutions might cause problems when used with optodes as these use optical signals for pH measurement.

Potential pitfalls

Pitfalls are associated with imprecise calibration and differences in the ionic composition of buffers and body fluids. Furthermore, air contact of samples must be minimised as loss of CO₂ from body fluids and associated pH shifts will occur. Both the calibration and sensor readings are temperature-dependent. Precise temperature control is therefore critical to perform accurate measurements of pH. Calibration of the electrode and analyses of samples should therefore be carried out at the incubation temperature of the organism. pH measurements in the body fluids of small animals (small sample volumes) are associated with the problem that a decrease in tip diameter of the sensor results in a decrease in sensitivity. With optodes, small fluorescent molecules, for example the degradation products of haemoglobin, interfere with the fluorescence-based measurement and could lead to a drift of the optode response preventing precise pH determination. This problem is not easy to solve and may require improved optode design.

9.3.2 *In vivo* magnetic resonance imaging (MRI) and spectroscopy (MRS)

In vivo ³¹P-NMR spectroscopy is most suitable for non-invasive determinations of intracellular pH (Moon & Richards, 1973; Kinsey & Moreland, 1999). Such measurements have been carried out in tissues and whole organisms, ranging from plants, invertebrates and insects to fish and mammals, including marine invertebrates and

fish (Bock *et al.*, 2002, 2008; Bailey *et al.*, 2003; Melzner *et al.*, 2006). The position of the inorganic phosphate signal (P_i) within the ³¹P-NMR spectrum (Figure 9.3) is most commonly determined and used for intracellular pH calculations. The chemical shift of any nuclear magnetic resonance of compounds in fast-exchange protonation/deprotonation equilibria depicts the effect of pH according to a modified Henderson-Hasselbalch equation:

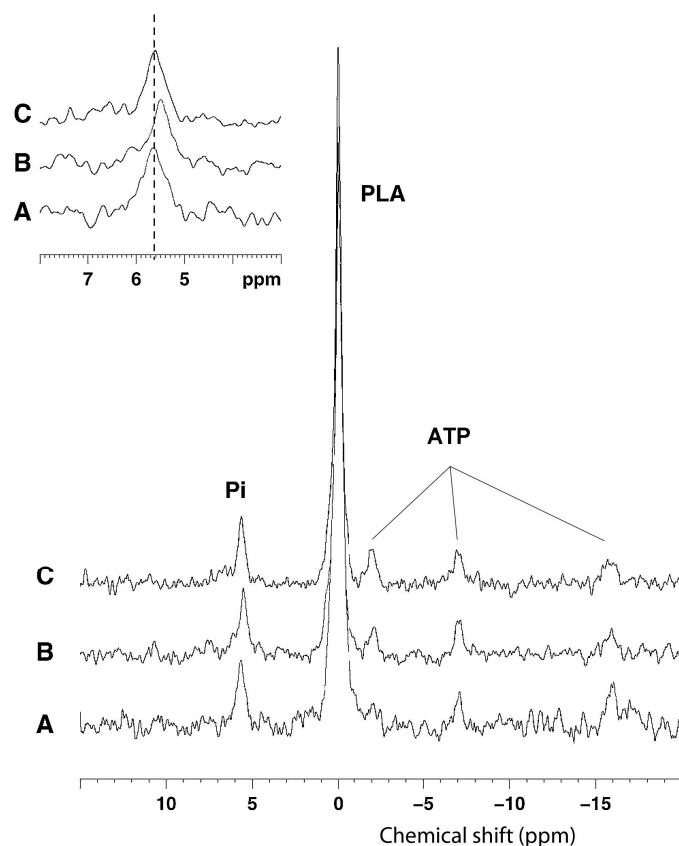
$$\text{pH} = \text{p}K'_a + \log_{10} \left[\frac{\delta_{\text{pi}} - \delta_{\text{ac}}}{\delta_{\text{ba}} - \delta_{\text{pi}}} \right]. \quad (9.4)$$

$\text{p}K'_a$ is the apparent dissociation constant of inorganic phosphate and δ_{ac} and δ_{ba} are the chemical shifts of protonated and deprotonated inorganic phosphate, respectively. Usually these parameters are determined empirically when measuring the chemical shift of the inorganic phosphate signal (δ_{pi}) relative to a pH-independent reference (such as the phosphate resonance in the phosphagen, e.g. phospho-L-arginine). Calibration is performed using model solutions of known pH simulating the cytoplasm of the species to be investigated.

Strengths and weaknesses

The use of inorganic phosphate as an endogenous pH indicator may be one of the most elegant ways to monitor changes in intracellular pH non-invasively, but there are a couple of drawbacks. The chemical shift of inorganic phosphate is influenced by factors other than pH, for example by temperature (Kost, 1990), protein concentration and free ion content (Roberts *et al.*, 1981). Calibration must be carried out for each species and experimental condition to avoid measurement errors. The model solution needs to reflect the cytoplasm of the species of interest. A careful analysis of the intracellular ionic strength and divalent cation concentrations can lead to an absolute accuracy of pH determination within ± 0.05 pH units (Roberts *et al.*, 1981; Madden *et al.*, 1991). Relative changes can be determined with accuracy better than ± 0.02 pH units. ³¹P-NMR spectroscopy is a rather insensitive technique requiring good signal to noise ratios of *in vivo* spectra for a precise determination of the chemical shift of the free inorganic phosphate signal. A minimum tissue fresh mass is required for good

Figure 9.3 *In vivo* ³¹P-NMR spectra recorded in isolated body wall muscle tissue from *Sipunculus nudus* at extracellular pH 7.9, under control conditions (A), 20 min after the addition of 2% CO₂ (P_{CO₂} = 1.97 kPa or 20,000 μatm) (B) and when the intracellular acidification was reversed after 10 h (C). P_i, inorganic phosphate; PLA, phospho-L-arginine; ATP, adenosine triphosphate. The inset shows the chemical shift of inorganic phosphate for A, B and C and the position shift with respect to PLA induced by changes in intracellular pH.



signal to noise ratios. However, the phosphate signal is not always detectable, for example in resting tissues of agile marine animals like cephalopods and fish (Bock *et al.*, 2002; Melzner *et al.*, 2006b), studied under conditions supporting standard metabolic rate (Sartoris *et al.*, 2003).

Potential pitfalls

Unfortunately, inorganic phosphate is not applicable as an extracellular indicator of pH, because of its critically low concentrations and the usually larger differences between pH_e and pK_a in the extracellular space.

Suggestions for improvements

The use of extracellular pH markers in both NMR spectroscopy and MR imaging has been described (for a review see Gillies *et al.* (2004)), but these substances have not yet been used in ocean acidification research. For instance, 3-Aminopropylphosphonate (3-APP) is a nontoxic, membrane-impermeable ^{31}P -NMR marker, with a pH sensitive chemical shift of 1 ppm per pH unit. This indicator was successfully used for the determination of pH_e values in tumours of mice (Gillies *et al.*, 1994). pH_e and pH_i were monitored in parallel from *in vivo* ^{31}P -NMR spectra, over a time course of about an hour. However, the limited sensitivity of ^{31}P -NMR enables measurements of pH_e only in large tissue volumes. An improvement in spatial resolution was achieved when imidazoles were introduced as extrinsic pH_e indicators. Van Sluis *et al.* (1999) compiled pH_e recordings in breast cancer tumours with a spatial resolution of $1 \times 1 \times 1 \text{ mm}^3$ using 2-imidazol-1-yl-3-ethoxycarbonyl-propionate (IEPA) and ^1H magnetic resonance spectroscopic imaging (^1H -MRSI). Recently, localisation and temporal resolution could be improved further using either relaxation enhanced pH measurements involving gadolinium-based contrast agents as extracellular pH markers (Garcia-Martin *et al.*, 2006) or magnetisation transfer techniques (Zhou *et al.*, 2003). All these approaches have their specific benefits and drawbacks. Which technique is most suitable primarily depend on the type of application. For each of these substances to be used in a specific organism, tissue or cell preparation it must be demonstrated that the substance remains in the extracellular space and does not exhibit significant biological activity.

9.3.3 Common fluorescent indicators of intracellular pH

Fluorescent pH indicators for monitoring cytosolic pH have been applied extensively in a wide range of cell types, primarily in cultured mammalian cells. A large literature base exists covering most aspects of their use. The most comprehensive description of the commonly used fluorescent pH indicators is provided by Haugland *et al.* (2005, Molecular Probes, The Handbook, at www.probes.com).

The majority of fluorescent pH indicators are derivatives of fluorescein which displays pH-dependent fluorescence shifts. The use of fluorescein to monitor intracellular pH has been described in detail by Kotyk & Slavik (1989). Fluorescein can easily be loaded into cells in the form of diacetate ester (FDA). Intracellular esterases hydrolyse the ester to release the ionic, pH-sensitive fluorescein. A major drawback of fluorescein is that it leaks easily from cells. The use of carboxyfluorescein reduces cell leakage although the pK_a of carboxyfluorescein is around 6.5, which is rather low for strong responses to cytosolic pH (around 7.3, species and tissue specific, falling in the warmth, increasing in the cold). Rink *et al.* (1982) introduced BCECF-AM, a membrane permeable, hydrolysable ester (2',7'-bis(carboxyethyl)-5,6-carboxyfluorescein; Figure 9.4), as an intracellularly trappable fluorescent pH indicator with an appropriate pK_a value and low leakage rates.

Convenience of handling and the opportunity of simultaneous investigations in many cells with a new dimension of spatial resolution led to rapid dissemination of this method. For the past 20 years, BCECF has been the main dye used for monitoring intracellular pH. It has a very high selectivity for H^+ and a pK_a around 7, close to cytosolic pH values. Moreover, the BCECF anion has up to 5 negative charges at physiological pH, which reduces its leakage from cells. BCECF can be loaded into most cells by incubation with the acetoxymethyl ester (AM) form. Intracellular trapping of the dye occurs once cellular esterases remove the AM group. Alternatively, membrane-impermeable free acid forms of the dye can be introduced into cells by microinjection (e.g. Gibbon & Kropf, 1994), through a patch clamp pipette or by electroporation or biolistics, as used for calcium indicators (Bothwell *et al.*, 2006). Cell impermeant forms can also be used to monitor extracellular pH.

Part 3: Measurements of CO₂-sensitive processes

SNARF and carboxy SNARF are two additional fluorescent dyes that are widely used to monitor intracellular pH. Carboxy SNARF has a pK_a around 7.5 and is therefore suitable for monitoring pH changes between 7 and 8. Variants of SNARF have a lower pK_a (around 7.2) and may be more suited to monitor pH changes at the lower end of the physiological range.

With new dyes (see below) and techniques, intracellular dye loading has been optimised by chemical modification. Expression vectors are available for dye synthesis within a transfected cell (Kneen *et al.*, 1998; Palmer & Tsien, 2006). Specific targeting of dyes into cytosolic compartments (Farinas & Verkman, 1999) and confocal laser fluorescence microscopy has further enhanced spatial resolution.

For a number of years, pHluorins, i.e. pH-sensitive forms of green fluorescent protein (GFP), have been used to monitor pH in intracellular compartments. This approach has the advantage of being essentially non-invasive since cells can potentially be genetically manipulated to express their own pH indicator. In addition to their use in monitoring cytoplasmic pH, pHluorins have the potential to be targeted to a range of cellular compartments. For example, a number of studies have used pHluorins targeted to the lumen of secretory vesicles providing highly sensitive monitoring of single cell secretory vesicle activity (Sankaranarayanan *et al.*, 2000).

pHluorins have the potential to provide long-term ratiometric monitoring of intracellular pH (e.g. Michard *et al.*, 2008). Calibration of pHluorins for monitoring cytoplasmic pH suffers from the same accuracy problems as the more conventional fluorescent indicators. So far, pHluorins have not been applied to any direct study of the effects of ocean acidification. Their application is currently limited by the availability of genetic transformation systems. A potential benefit of pHluorins that is particularly relevant to ocean acidification studies is that they should be suitable for monitoring intracellular pH during long-term experiments.

Prior to the experiment, viable cells or small tissue preparations (Bleich *et al.*, 1995) are incubated for about 20 min with BCECF-AM (1 to 10 μ M). BCECF becomes more concentrated with time and the majority of the dye is located in the cytoplasm. Illumination of BCECF by blue light (e.g. 488 nm) induces a green fluorescence (emission maximum 518 nm). The fluorescence intensity of the emitted (green) light is characteristically decreased by an increase in H⁺ activity. If the dye is illuminated at 436 nm the emission intensity is lower and independent of pH (isosbestic point at 439 nm). This property enables ratiometric monitoring of intracellular pH independent of dye concentration. Figure 9.5 shows the intensities of the green fluorescence detected at 535 nm while pH is varied between 6.2 and 9.5. SNARF and carboxy SNARF dyes exhibit shifts in both their excitation and emission spectra, potentially making them more versatile for a range of optical systems.

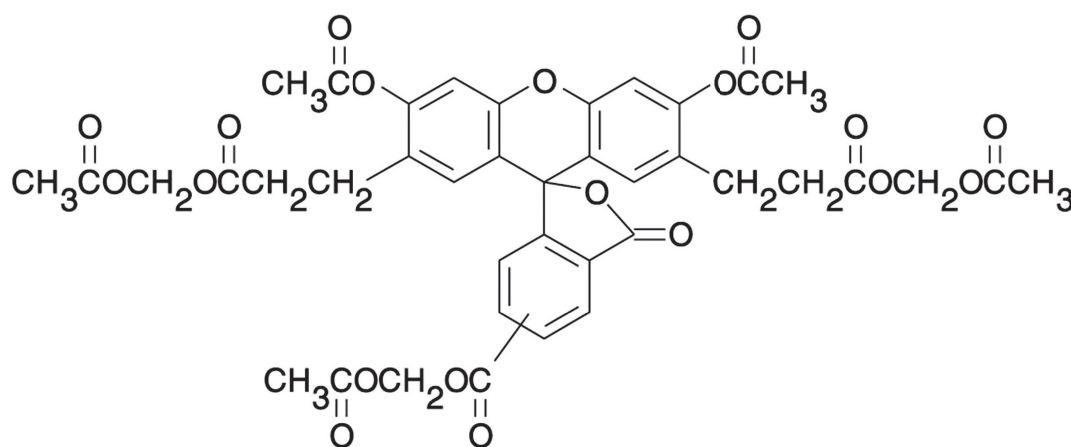


Figure 9.4 Chemical structure of the BCECF-AM, an ester derivative of carboxyfluorescein which is membrane permeable and intracellularly hydrolysable. Modified from <http://probes.invitrogen.com>.

In particular, the emission spectrum shift makes these dyes more suited for confocal studies with single laser excitation (488 nm). The ratio of emission at 630 and 590 nm is pH-dependent. pH-sensitive fluorescent dyes may also be used in combination with other ion indicators (e.g. the calcium indicator fura-2) that have different excitation or emission properties.

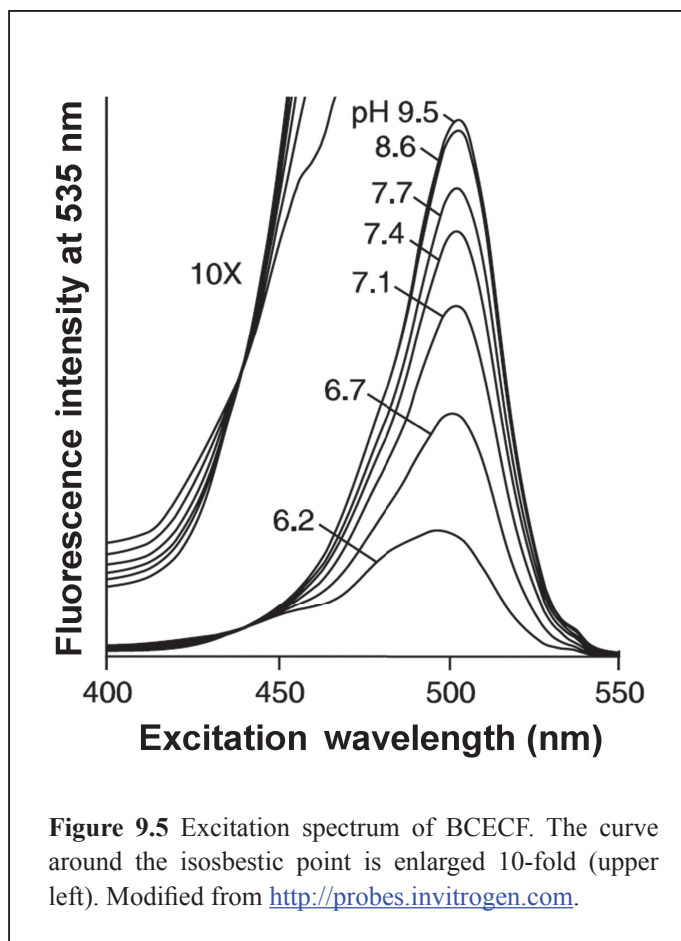
The light from conventional sources (mercury or xenon lamp) is focused to a beam and the excitation wavelength is selected. After appropriate attenuation of the intensity by grey filtering, the beam is mirrored into the light path of the microscope in direction to the preparation. A dichroic mirror reflects the excitation light to the object and transmits the emission light on its way back to the detection system. For BCECF studies, a bandpass filter in the emission pathway selects the emission wavelength around 520 nm. Computer controlled selection of excitation wavelengths, either by a bandpass filter wheel or by a grid-based monochromator system, enables the alternating illumination of the cells at 436 and 488 nm. The data are collected by a photon counting tube or to a CCD camera as photon counts or pixel intensities. The phototube allows detection of very low signals at high time resolution while the CCD camera is slower and has a better spatial resolution. The highest spatial resolution is provided by confocal microscopy and a variety of laser lines (argon, helium-cadmium) are available to cover the excitation spectrum of BCECF.

During the experiment, the dye concentration falls due to photobleaching and cellular export. Hence, the fluorescence intensity follows this decline and cannot be used directly as a pH signal. Since the pH-dependent change of fluorescence intensity does not occur at 436 nm excitation, the ratio of emission intensities at 488 nm/436 nm excitation is calculated as a concentration-independent indicator of intracellular pH.

In order to translate the ratio values into H^+ activity, a calibration procedure must be performed *in situ* (Thomas *et al.*, 1979). Nigericin, an ionophore for K^+ and H^+ , is used to permeabilise the cell membrane and pH is calibrated by extracellular solutions of defined pH. The composition of calibration solutions must mimic the cytosol in order to prevent the generation of a diffusion voltage which otherwise would bias the H^+ activity inside the cell. Alternative calibration methods are discussed in Eisner *et al.* (1989).

An attractive approach to cellular acid-base physiology is the combination of patch clamp technique and fluorescence microscopy. Dye loading can be directly performed via the patch pipette which gives access to the cytosol. In this way, functional signals occurring in parallel to the changes in pH_i can be monitored. In addition, dextran-coupled BCECF is available with even better properties with respect to dye compartmentalisation. Its distribution is restricted to the cytosol and it displays very low leakage out of the cell.

An interesting aspect of pH measurements to investigate membrane transport and H^+ homeostasis is the experimental modification of pH_i . In principle, every membrane-permeable weak acid or base can be used to transiently modify pH_i at constant extracellular pH. Buffers like NH_3/NH_4^+ , propionic acid/propionate, acetic acid/acetate, and CO_2/HCO_3^- are frequently used. Figure 9.6 shows an example for CO_2/HCO_3^- and NH_3/NH_4^+ .



Part 3: Measurements of CO₂-sensitive processes

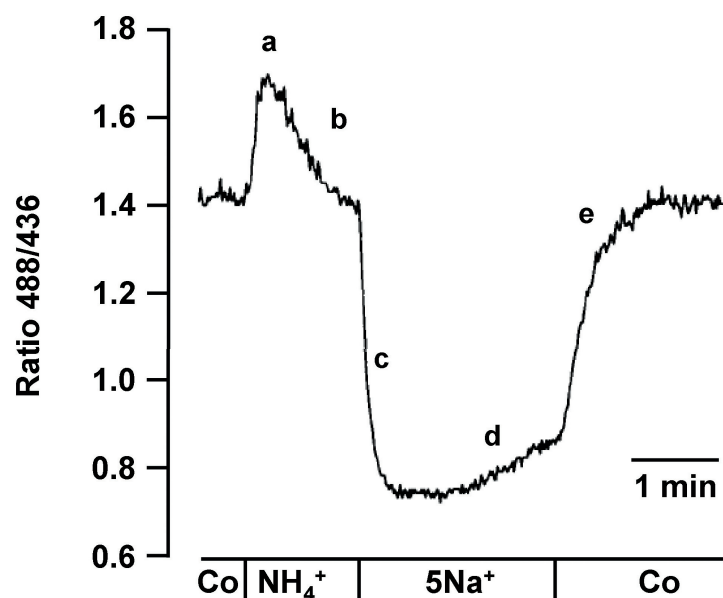
Normally, CO₂ is in equilibrium with HCO₃⁻ and H⁺. For pH measurements this would mean that it is impossible to distinguish between the effects of CO₂ and HCO₃⁻ on physiological processes. The challenging part in pH experiments involving CO₂/HCO₃⁻ buffers is therefore to alter the CO₂ concentration at constant levels of HCO₃⁻ and pH. Although this seems to be contradictory to the Henderson-Hasselbalch equation, this approach is experimentally feasible. It makes use of the slow time constant for the generation of carbonic acid which is necessary to reach a new equilibrium after a change in one of the components. The method involves the acute mixing of two buffer solutions which immediately perfuse the cells under investigation (Zhao *et al.*, 1995; Figure 9.7).

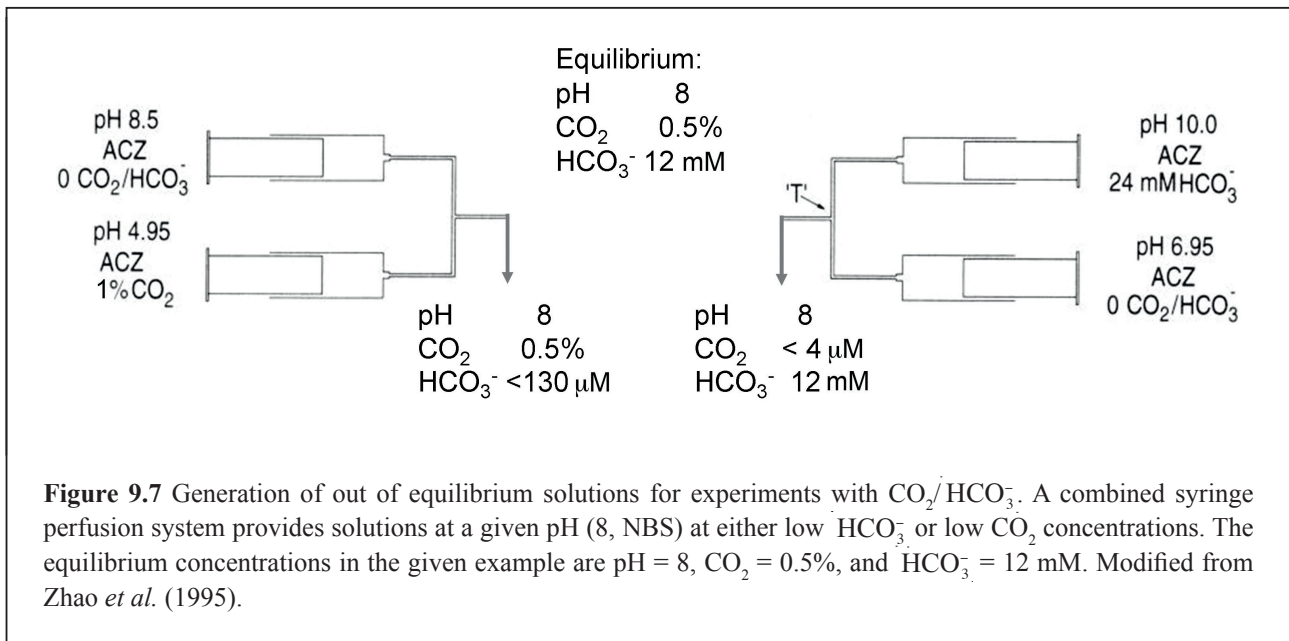
Strengths and weaknesses

pH_i measurements by fluorescent dyes such as BCECF are robust and easy to perform. The approach is almost non-invasive and the signal obtained, even without spatial resolution, reflects cytosolic pH. The auto-fluorescence signal at the given excitation wavelengths of BCECF is low and does not limit the measurements even when dye loading is weak. There are calibration methods available which provide reasonable precision in interpreting the ratiometric data.

The overriding advantage of fluorescent indicators is that they are often the only method available for monitoring intracellular pH in individual small cells that are not tractable for microelectrode measurements. With respect to resolution, they also have clear advantages over bulk measurement methods when a small number of cells are available. Fluorescent indicators are less useful for monitoring pH in single cells within tissues due to optical problems associated with thick tissue. The use of AM ester loading can be considered to be minimally disruptive, given certain assumptions about the concentration of the dye. However, since pH dyes essentially act as pH buffers, loading too high intracellular concentrations may exert significant buffering around the pK_a of the dye, possibly even enough to overcome the pH buffering mechanisms of the cells. In practice, this may be minimised by having a low concentration of dye in the loading solution (typically 1 to 10 μM) and by carefully controlling the loading time. Acetoxymethyl esters have low solubility in water and need to be prepared as stock solutions, normally 1 mM in dimethyl sulfoxide (DMSO). The incubation period, especially if performed in the presence of membrane permeabilising

Figure 9.6 Effect of changes in pH_i by the NH₃/NH₄⁺ and Na⁺ dependence of cellular compensation of the respective acid load (modified from Bleich *et al.*, 1998). a) Perfusion of a 20 mM solution of NH₃/NH₄⁺ initially results in cellular alkalinisation (NH₃ enters the cell and buffers H⁺, NH₄⁺ does not permeate the cell membrane). b) The cell recovers from the alkaline load with a certain time constant, for example by acid/base transport. c) Removal of NH₃/NH₄⁺ from the perfusion results in cellular acid load (NH₃ leaves the cell and H⁺ is left behind). d) Cellular acid load is compensated by acid/base transport. The rate of recovery in this case depends on extracellular Na⁺. The rate is low at low concentration of Na⁺ (5mM; d) and high at high Na⁺ concentration (145mM; e).





agents or detergents, takes place in non-physiological conditions which may cause irreversible changes to the investigated cells. Photobleaching of dye and cytosolic material limits the intensity of the excitation light or the duration of the excitation. At high intensities, light can cause significant heat damage to the cells. Although calibration is easy as long as there is a stable fluorescence ratio, i.e. as long as there is no significant background fluorescence or specific light absorption, the calculation of H⁺ fluxes across the cell membrane requires the determination of the cytosolic buffer capacity, which is more difficult. Finally, the technique always implies a trade-off between time resolution and spatial resolution.

The BCECF and SNARF dyes share the advantage that they can be used in ratiometric mode. Both have been used extensively for imaging applications to individual cells in a variety of microscopy modes. Their use may also be combined with cell electrophysiology such as patch clamp (e.g. Trapp *et al.*, 1996). Measurements in individual cells are also possible using micro-photometry to record average intracellular pH values for single cells or small numbers of cells. Both the BCECF and SNARF dyes have been used with flow cytometry to gain information on the pH of cells maintained in culture (e.g. Musgrove *et al.*, 1986). They could potentially be used with natural populations of unicellular organisms, including phytoplankton.

The appropriate choice of a fluorescent dye depends on the cell type under study, the range of pH values to be monitored, the type of physiological response expected and, not the least, the recording apparatus available. In our experience, BCECF has certain advantages over SNARF for the measurement of intracellular pH in marine microalgae. Most cell types (including coccolithophores and diatoms) load particularly well with BCECF-AM, requiring loading periods of less than 30 min with 5 μM loading solution. The relatively wide separation of excitation wavelengths (450 and 480 nm) means that relatively broadband excitation (>10 nm bandpass) is possible. However, the dual excitation properties of BCECF limit its use to systems with dual wavelength excitation, either with a filter changer or monochromator for wide field studies or dual laser excitation for confocal or flow cytometry (e.g using the 488 and 458 nm excitation of an argon ion laser). SNARF and carboxy SNARF offer the advantage of ratiometric emission indicators which can be used with a single wavelength excitation source (normally 488 nm). Optimal emission wavelengths are around 640 and 585 nm. A significant limitation of the use of SNARF and carboxy SNARF is that, while higher overall fluorescence signals are obtained with a 488 nm excitation, the relative emission peaks are considerably different at physiological pH around 7.2 with very low fluorescence at 590 nm. This can be overcome by exciting at 530 nm but with an overall reduced fluorescence yield. A further limitation with the use of SNARF is the proximity of the longer emission wavelength to the fluorescence emission

Part 3: Measurements of CO₂-sensitive processes

of chlorophyll. Therefore, light must be collected from a relatively narrow emission band with further reduction in signal. In small cells, such as the coccolithophore *Emiliana huxleyi*, the signal to noise ratio of SNARF may be limiting for useful measurements (Berry, 2001).

Dye bleaching is a significant limitation to the use of BCECF and SNARF dyes in individual cells and may limit measurements to a relatively short time period (typically a few minutes), depending on the type and intensity of the excitation. Dye bleaching is particularly problematic with smaller cells, where there is a limited pool of unbleached dye to replace the dye bleached in the region or focal plane of excitation.

A well-recognised problem with the majority of fluorescent ion indicators is dye compartmentalisation. Accurate measurement of cytoplasmic pH is the goal of many studies using fluorescent pH indicators. However, the dye can be compartmentalised into subcellular organelles and vacuoles, either by diffusion of the undissociated AM ester or by direct translocation of the free anion by membrane transporters. Compartmentalisation can be identified by the appearance of punctuate fluorescence and a drifting ratio signal as dye enters more acidic or alkaline compartments. The time course and extent of compartmentalisation may strongly depend on the cell type. In short-term experiments this may not be problematic. Compartmentalisation may be overcome by the use of dextran-conjugated indicators (both BCECF and SNARF are available as high molecular weight dextran conjugates). However, this requires loading of the dextran conjugate into the cell by disruptive procedures such as microinjection or biolistics. The combined effects of bleaching, compartmentalisation and dye extrusion generally lead to reduced dye signal during the course of an experiment and therefore fluorescent pH indicators are generally not suitable for long-term measurements.

The pH sensitivity of BCECF or SNARF may be better than 0.05 pH units in ideal solutions. However, the accuracy of pH measurement is far less certain due to uncertainties associated with intracellular calibration of the dye. Indeed, calibration is the major limitation of the use of fluorescent intracellular ion indicators. Accurate calibration of intracellular pH indicators presents a particular set of problems. The pK_a of fluorescent pH indicators is affected by the ionic strength of the solution. Extracellular calibration in pH-buffered solutions with ionic strength adjusted to mirror that of the cytosol may partially overcome this limitation. However, other cellular factors may significantly influence the behaviour of the dye. These include cytosolic viscosity (Poenie, 1990), the presence of other pigments (e.g. chlorophyll) that may preferentially absorb different excitation wavelengths of BCECF and the presence of autofluorescent pigments. For accurate monitoring of intracellular pH in dye-loaded cells, it is necessary to be able to clamp the pH of the intracellular compartment under study to a known value. The H⁺ ionophore nigericin has been widely used to achieve control of cytosolic pH. Nigericin creates pores that allow the exchange of H⁺ with K⁺. In an ideal experiment, this overrides the cell transport processes, allowing the equilibration of K⁺ and H⁺ fluxes across the membrane and will clamp cytosolic pH according to the intracellular and extracellular concentrations of K⁺ according to the equation:

$$\frac{[K_{in}^+]}{[K_{out}^+]} = \frac{[H_{in}^+]}{[H_{out}^+]} \quad (9.5)$$

In practice, $[K_{out}^+]$ is set to approximate $[K_{in}^+]$ (100 to 200 mM) so that $pH_{out} = pH_{in}$. It follows that accurate clamp of intracellular pH requires a good knowledge of $[K_{in}^+]$. While this approach has been used in a large number of studies, including with marine phytoplankton (Dixon *et al.*, 1989), it is recommended to perform an additional calibration procedure such as by the use of weak acid and base treatments to achieve maximum and minimum fluorescence ratios corresponding to H⁺-saturated and H⁺-free forms of the dye (James-Kracker, 1992).

The use of fluorescent indicators in ocean acidification studies is clearly best suited to monitor changes in pH in short-term physiological experiments aimed to better understand pH regulatory mechanisms. In such studies, fluorescent indicators can give relatively high precision measurements with excellent spatial and temporal resolution. Their applicability to accurate assessment of resting pH or for monitoring long-term changes in intracellular pH is limited due to a range of factors that tend to result in dye loss and difficulties with accurate calibration.

Potential pitfalls

Potential cell damage by tissue preparation and incubation can occur and is not necessarily visible in the fluorescence results. Additional functional testing of cells under investigation is strongly recommended. Since BCECF-AM is lipophilic, the pigment is dispersed rather than dissolved and requires addition of DMSO as a detergent. A reasonable level of dispersion is only obtained if the stock solution is pipetted directly into a large volume of experimental solution rather than the other way around. Overloading of cells with dye leads to additional cytosolic buffering and the pH is clamped. On the other hand, only efficient dye loading enhances the signal to noise ratio. This is especially relevant for BCECF since the emission at 436 nm excitation is weak (Figure 9.4). There are a variety of cells which express transporters for organic anions which bind and remove the dye from the cell at high transport rates (e.g. renal proximal tubule cells).

In imaging experiments, one should carefully follow and understand the calculation procedures of the imaging software, which finally results in the fluorescence ratio value for a selected region of interest. Background noise and selected intensity thresholds might influence these values significantly. Measurements outside the experimental pH range, given by the pK_a of the dye, means leaving the range of linear relations between the fluorescence ratio and pH. No quantitative measurements can be performed outside this range. The most interesting information on cytosolic pH regulation is derived from time constants for the recovery of pH_i after experimental manipulation. The precision of such data strongly depends on the flow of the medium bath and on exchange rates in relation to the kinetics of the transport mechanisms under investigation. It is strongly recommended to monitor the successful equilibration of the CO_2 solutions and to ascertain that the temperature is constant.

Suggestions for improvements

All factors influencing the preparation as well as the measurement itself should be optimised for a given tissue preparation. In some cases it is feasible to invest into the generation of cell cultures with defined properties, dependent on the availability of native material. Cell cultures also enable experimental approaches at larger scales and to target genes of interest.

9.3.4 New fluorescent indicators of intracellular pH

Ageladine A is a brominated pyrrol-imidazole alkaloid, which was first isolated and described by Fujita *et al.* (2003). The dye was found in extracts of the sponge *Agelas nakamura* by using bioassay-guided fractionation. The substance shows biological activity which involves the inhibition of matrix metalloproteinases and of cell migration of bovine endothelial cells. Meketa & Weinreb (2006) and Shengule & Karuso (2006) completed the synthesis of ageladine A, which was later optimised by Meketa & Weinreb (2007) and Meketa *et al.* (2007). Bickmeyer *et al.* (2008) described its fluorescence spectra and pH-dependency as well as its application as a dye in isolated cells and transparent animals.

Ageladine A is brominated and can be protonated on the guanidine moiety, which stabilises the molecule in two forms. Maximum fluorescence is at 415 nm under excitation with UV light (365 nm) with a broad emission spectrum up to more than 500 nm (Figure 9.8). Fluorescence changes of ageladine indicate pH values in the range between 4 and 9, with a half maximal pH of 6.26. UV excitation ranges from 325 to 415 nm with an excitation maximum at 370 nm. Dye concentration influences fluorescence; hence, the calculation of pH requires calculation of the concentration using a calibration curve. A rough pH estimate can be obtained from the fluorescence intensity derived from the ratio at excitations of 340 and 380 nm. At higher dye concentrations, this two-wavelength approach reduces the concentration dependency of the measurements. In cells and membranes, ageladine A concentrations are usually unknown and may only be estimated from its concentration used during incubations. In a standardised procedure, cells or tissues are loaded with 10 μ M ageladine A for 10 min, whereas 30 min are required in whole animal procedures. Small pH changes are best monitored by excitation at 370 nm and emission at >415 nm or using the Fura 2 filter settings (340/380 exc.). The calculation of exact pH values can only be obtained if the dye concentration is known, which is hardly feasible in living cells and tissues.

Strengths and weaknesses

Ageladine A, because of its bromination, easily passes membranes and can therefore be used to stain single cells as well as whole animals or organs. It is best to use in transparent aquatic animals. The use of a UV fluorescent microscope with whole animals allows to easily spot specific tissues. We presently think that only acidic tissues and cells become fluorescent, because ageladine A shows weak or no fluorescence at pH 8 to 9. pH changes can be monitored with high sensitivity, but for exact pH values, the actual dye concentration has to be known. This is the most critical point, because it is very difficult or nearly impossible to know the exact concentration of the dye at the site of the measurement in living tissue. Current research investigates whether the dye accumulates in cell membranes and whether it is stabilised when protonated. A major advantage of ageladine A is its emission at 415 to 430 nm where autofluorescence is very low. This considerably increases the signal to noise ratio compared to other pH-sensitive dyes with emissions at longer wavelengths.

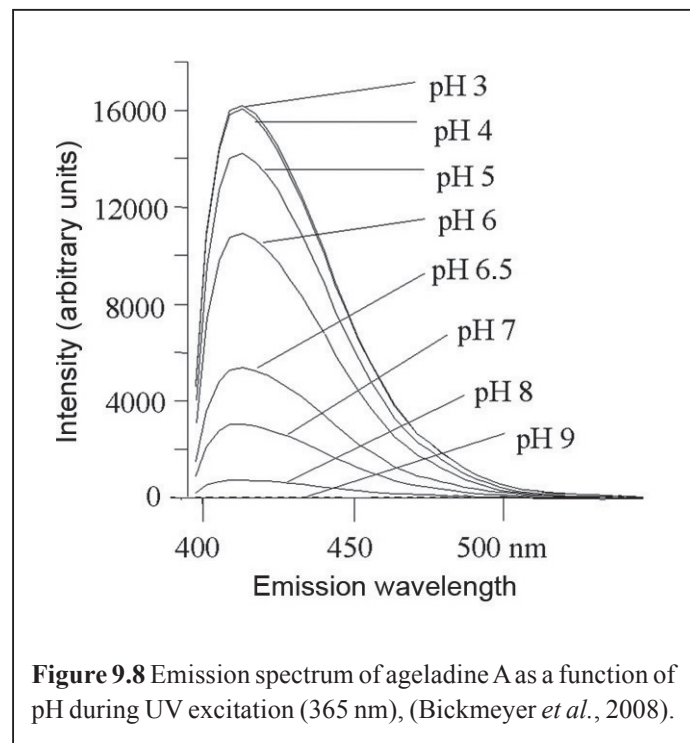
Potential pitfalls

At the moment it is not known whether ageladine A interacts with divalent ions or other molecules to produce false positive results. If it accumulates in cellular membranes, the pH sensitive guanidine moiety should be directed towards the cytosol and track pH changes. It remains to be explored whether some of the guanidine moieties are directed outwards and respond to extracellular pH. In that case, local pH changes close to the membrane may lead to erroneous estimates of bulk changes in pH.

9.3.5 Homogenate analyses of intracellular pH

The mean pH_i of tissues can be determined by the homogenate method (Pörtner *et al.*, 1990). The homogenate technique allows for a clear allocation of mean intracellular pH values in tissues to the experimental condition of the animal. It eliminates time delays in pH_i assessment associated with other techniques (delays caused by diffusion limitation, delayed equilibration between compartments or the necessity to accumulate recordings to improve the signal to noise ratio). The method follows the freeze-stop technique, which had been established for determining the metabolite status of shock frozen tissues (Wollenberger *et al.*, 1960). Since tissues can be stored away under liquid nitrogen until analysis the method is applicable to samples collected in the field.

Tissue samples are ground in liquid nitrogen using a mortar and pestle, and the tissue powder is then thawed in a medium containing potassium fluoride (KF) and nitrilotriacetic acid (NTA). The volume of medium is about 5 times the wet weight of the tissue; for example, about 100 mg of tissue powder are placed into 600 µl of ice-cold medium (160 mM KF, 1 mM nitrilotriacetic acid, pH 7.4). KF and NTA remove the Mg²⁺ and Ca²⁺ ions and prevent ATP-dependent metabolism, which occurs through the action of Mg²⁺ and Ca²⁺-dependent ATPases and kinases. The concentration of NTA is minimised to avoid proton release during its binding of Mg²⁺ and Ca²⁺. It is set just high enough to minimise the metabolic activity of the tissue. After completely



filling the vial with medium, the mixture is stirred with a needle in order to release air bubbles. It is then mixed vigorously and centrifuged for 30 s. In the original procedure the pH of the supernatant is measured using a Radiometer glass capillary pH electrode (G299A). pH microelectrodes and more recently, pH optodes, have also been used successfully (Krause & Wegener, 1996; T. Hirse & H.-O. Pörtner, unpublished). The resulting value approaches pH_i with an experimental error of less than 0.01 pH units (Pörtner *et al.*, 1990). According to model calculations (Pörtner *et al.*, 1990), any distortion in the measured pH values due to either the pH of the medium, dilution by the medium or mixing with intra- or extracellular fluids can be disregarded. The accuracy of the method for each individual pH measurement is confirmed by the strong correlation of pH_i changes with changes in metabolic parameters (Pörtner *et al.*, 1991a, 1996). See Pörtner (1987a, 1995) for details on how the metabolism shapes the pH response and influences non-bicarbonate buffering.

Strengths and weaknesses

The homogenate technique determines intracellular pH in tissues with much less signal to noise ratio than methods using dimethyl-oxazolidine-dione (DMO) (see below), ^{31}P -MRS or fluorescent dyes. The homogenate technique shows a variability one order of magnitude lower and a level of precision and accuracy one order of magnitude higher than the DMO technique (Pörtner *et al.*, 1990), which is therefore rarely used nowadays.

The homogenate technique is the only method that includes the quantitative contribution of all cell and tissue compartments to mean cellular pH and in response to acid-base disturbances, with an emphasis on cytosolic pH (see below). For successful analysis, the resting and experimental states of the tissues must be maintained during invasive sampling. Experimental animals may have to be anaesthetised prior to tissue sampling and decapitated to eliminate a potential stress response (Pörtner *et al.*, 1990, 1991a,b; Tang & Boutlier, 1991). The main merits of the homogenate technique are the simple methodological procedure, low cost, low variability and the small sample size required (as low as 20 mg fresh weight). The method can be used with samples collected from active animals or even from animals collected in the field. The latter is especially relevant in the context of investigations of ocean acidification *in situ*. The main drawback of the method is that it only allows point measurements as the organism is sacrificed.

Potential pitfalls

CO_2 condensation into the liquid nitrogen and onto pre-cooled instruments may cause acidification of the samples and must be minimised during the preparation of the homogenate. The use of clean liquid nitrogen and dewars, mortars and pestle free of rime is required. A short but efficient grinding procedure under a nitrogen atmosphere excludes contamination with condensating CO_2 . It is usually sufficient to grind on the bottom of a box, for example a Styrofoam box, allowing the evaporating nitrogen to fill up the volume above the mortar and pestle. pH is best measured in a thermostatted capillary pH electrode, after preparation and centrifugation of the homogenate in a closed Eppendorf cap (usually 0.5 ml, volume to be reduced with small sample size). If required, complete tissue extraction can be ensured using ultrasound. The pH electrode and supernatant (e.g. inside the capillary electrode) must be thermostatted at the experimental temperature of the animal in order to avoid artefacts. Nitrioltriacetic acid (NTA) rapidly binds calcium and magnesium ions and thereby stops metabolism. At the same time, its concentration needs to be minimised since it releases protons during the binding process. An excess of fluoride in the reagent solution minimises proton release from NTA due to the formation and precipitation of magnesium or calcium fluorides.

9.3.6 Analyses of non-bicarbonate buffer values

The *in vivo* response of buffers to disturbances of the acid-base equilibrium comprises closed (no exchange with other compartments) and open system (substances such as CO_2 can be exchanged) characteristics. The CO_2 /bicarbonate buffer reaches high values in an open system (when Pco_2 is maintained and CO_2 generated by the acid titration of bicarbonate is released). Such CO_2 /bicarbonate buffering in open systems is relevant especially in animals with high internal Pco_2 levels. Accordingly, the bicarbonate buffer needs to be distinguished from non-bicarbonate buffers (mostly protein and inorganic phosphate).

Part 3: Measurements of CO₂ - sensitive processes

Determinations of tissue non-bicarbonate buffer values by tonometry (Heisler, 1989; Pörtner, 1990a) use CO₂ for the titration of buffers and thereby mimic the respiratory changes in the acid-base status *in vivo*. Changes in the bicarbonate levels associated with CO₂-driven changes in pH reflect the involvement of non-bicarbonate buffers (Heisler & Piiper, 1971; cf. Figure 9.1).

The non-bicarbonate buffer value ($\beta_{NB} = -\Delta[\text{HCO}_3^-]_e / \Delta\text{pH}_e$) of the extracellular fluid (whole blood, haemolymph and coelomic fluid) is typically determined by CO₂ equilibration using an intermittently rotating cuvette (tonometer model 273, Instrumentation Laboratory, Paderno Dugano, Italy) flushed with a humidified mixture of CO₂ in air (between 0.2 to 1%) provided by a gas mixing pump (Wösthoff, Bochum, Germany). The samples of haemolymph are tonometered for 25 min to allow equilibration and are then analysed for pH and total CO₂ content C_{CO₂} as described below.

Tissue non-bicarbonate buffer values are best determined using the homogenate technique under metabolic inhibition. This method yields values under control conditions as required for quantitative treatments, i.e. the pH/bicarbonate analysis of proton quantities underlying observed changes in acid-base parameters (e.g. Pörtner, 1990a; Pörtner *et al.*, 1991a, b; Ferguson *et al.*, 1993). Initially, intracellular buffer values $\beta_{i(NB, NP)}$ (non-bicarbonate, non-phosphate buffer values) of tissues are determined (Pörtner, 1990a). In brief, tissues are powdered under liquid nitrogen, samples of tissue powder are then placed into preweighed tonometer vessels containing an ice-cold solution composed of 540 mM KF and 10 mM nitrilotriacetic acid (1:3 w:v). Homogenates are tonometered under humidified gas mixtures between 0.5 to 4% CO₂ in air in the order medium to low (high) to medium to high (low) CO₂ (Heisler & Piiper, 1971). After equilibration for 25 min, samples taken at each CO₂ level are rapidly centrifuged in a capped Eppendorf tube and the supernatants analysed for pH and C_{CO₂} as described below and for free inorganic phosphate as described by Pörtner (1990a). The intracellular buffer values of tissues are calculated by applying a correction for the dilution of the respective tissue and for extracellular space according to the following equation (Heisler & Neumann, 1980):

$$\beta_{i(NB, NP)} = (\beta_{(NB, NP)} \times V) + \frac{(F \times W)}{F \times W \times (1 - Q)}; \quad (9.6)$$

where $\beta_{i(NB, NP)}$ is in mmol pH⁻¹ kg⁻¹ wet weight, V is the volume of the medium, F is the fraction of tissue water, W is the blotted fresh weight and Q is the fractional extracellular volume. The buffer values of inorganic phosphate is added to this value according to free intracellular concentrations under resting conditions (about 1 mmol kg⁻¹ wet weight).

The water content of tissues is determined by drying at 110°C for 24 h. The extracellular space of tissues is determined after incubation in artificial seawater (invertebrates) or in a Ringer solution (fishes) in the presence of 0.1 µCi (0.037 MBq) per ml of ³H-inulin for 1 h. The tissues and perfusate are then deproteinised with 0.6 N perchloric acid and the ³H activity of the supernatant is measured with a liquid scintillation counter. The fractional extracellular volume (Q) of the tissue is calculated as the ratio of extracellular tissue water volume and total tissue water volume according to Heisler (1975).

Strengths and weaknesses

Invasive (homogenate technique) and non-invasive approaches (by ³¹P-NMR) for the determination of tissue buffer values yield similar values of β_{NB} (Wiseman & Ellington, 1989; Pörtner, 1989, 1990a). The homogenate technique requires high concentrations of KF for sufficient inhibition, which implies the need of correcting for changes in ionic strength of the medium as well as for the buffering effect of the accumulated inorganic phosphate.

Potential pitfalls

Regardless of whether buffer values are determined in intact tissue or homogenates, metabolic processes may respond to experimental changes in pH and may interfere with the measurements leading to erroneous pH values or the production of additional buffers during the titration (cf. Pörtner, 1989). Hence, the buffer value measured does not actually correspond to any definite physiological state of the tissue, and definitely not to

that of control conditions. Most published non-bicarbonate buffers are, therefore, erroneously high because cytosolic buffering is increased during the titration procedure in similar ways as during anaerobic exercise, due to the release of inorganic phosphate from phosphagen and ATP. Complete metabolic inhibition and continuous recording of pH during the titration procedure enable accurate analyses but correction for such metabolic shift is nonetheless required.

9.3.7 Analyses of total CO₂ in body fluids and homogenates

Partial pressure of CO₂ in body fluids is measured by CO₂ electrodes. The total CO₂ content (C_{CO₂}) of body fluids (equivalent to the total dissolved inorganic carbon (DIC) in chemical oceanography, plus CO₂ bound to some proteins such as haemoglobin) can be determined after release of gaseous CO₂ by addition of acid. Detection of the CO₂ released occurs by various methods, ranging from electrodes to infrared analyses, conductometric methods and gas chromatography (Cameron, 1986). Gas chromatography (Lenfant & Aucutt, 1966) has been adapted to work with small sample volumes (20 to 50 µl) and a high precision to about 0.05 mM (Boutilier *et al.*, 1985; Pörtner *et al.*, 1990). Alternatively, Corning 965 CO₂ analysers can be used to measure DIC or C_{CO₂} with an accuracy of about 0.1 mM on 50 to 250 µl fluid samples. Some authors have even reached an accuracy of 0.02 mM when analysing large sample volumes (250 µl) of mussel haemolymph and bracketing each sample with known bicarbonate standard (Booth *et al.*, 1984). Refurbished Corning CO₂ analysers are still available on the market (Olympic Analytic Service OAS, Malvern, UK) and are relatively inexpensive. These instruments are based on the release of gaseous CO₂ by mixing of a fluid sample with a lactic acid solution in a sealed chamber and subsequent CO₂ determination using a thermal conductivity detector.

C_{CO₂} of extracellular fluids should be measured after removal of cellular components by centrifugation. C_{CO₂} levels of intracellular fluids are analysed after tissue extraction, which leads to contamination by extracellular compartments, including interstitial fluids (cf. Pörtner *et al.*, 1990). For further evaluation of the CO₂-bicarbonate system, the physical solubility of CO₂, (α), and the apparent dissociation constant $pK^{\prime\prime}$ of carbonic acid for body fluids and seawater are calculated according to Heisler (1986). The calculation is very flexible as the constant can be adjusted to a wide range of ionic compositions, ionic strengths and protein levels in the various compartments. The concentration of the apparent bicarbonate concentration in extracellular plasma ($[HCO_3^-]_e$) is calculated from C_{CO₂} according to the equation:

$$[HCO_3^-]_e = C_{CO_2} - (\alpha_{CO_2} \times P_{CO_2}) \quad (9.7)$$

Note that the apparent bicarbonate concentration includes both the bicarbonate and carbonate species. See Pörtner *et al.* (1990) for a full set of equations.

Intracellular P_{CO₂} and bicarbonate levels

The analysis of pH_i and total CO₂ levels (C_{CO₂}) in the homogenate allows quantifying the cellular bicarbonate concentration and P_{CO₂}. The total CO₂ measured in the homogenate must be corrected for fractions of extracellular water and CO₂ content using an adequate marker for extracellular space (for example radiolabelled inulin) to derive intracellular C_{CO₂} levels (Pörtner *et al.*, 1990):

$$P_{iCO_2} = \frac{C_{CO_2}}{10^{pH_i - pK^{\prime\prime}} \times \alpha + \alpha} \quad (9.8)$$

The calculation of intracellular C_{CO₂} requires parameters analogous to those needed for the determination of intracellular pH from DMO (dimethyl-oxazolidine dione) distribution. Consequently, errors similar to those involved in the DMO approach arise (see below). The intracellular P_{CO₂} calculated from the intracellular total CO₂ concentration (Pörtner *et al.*, 1990, 1991a, b, 1996; Boutilier *et al.*, 1993; Reipschläger & Pörtner, 1996) exhibits a relatively large variability, which can be reduced by highly accurate estimates of intracellular pH as with the homogenate technique.

With adequate knowledge of the relationships between the intra- and extracellular pH, P_{CO₂} and bicarbonate levels, intracellular acid-base parameters in isolated muscle tissues could be varied and clamped by setting

adequate values in the extracellular medium (Reipschläger & Pörtner, 1996). Among all acid-base parameters only a decrease in extracellular pH was suitable to cause metabolic depression during environmental stress (Pörtner *et al.*, 2000). Further experimental, mechanistic, studies are needed to demonstrate the regulatory function of individual acid-base parameters. This will support the development of a cause and effect understanding beyond what can be provided by empirical or correlative analyses.

9.4 Compartmental measurements: towards a quantitative picture

9.4.1 Extracellular fluids

Coleomic fluid, haemolymph and blood

Seawater is the extracellular space for unicellular organisms and the original extracellular fluid of marine animals. Accordingly, the body fluids of most marine invertebrates display ion compositions similar to those of seawater. In echinoderms, the extracellular fluid is (still) in contact with seawater, indicating that changing the ion composition or the acid-base status of these fluids through ion exchange processes only occurs within narrow limits.

The study of extracellular acid-base status requires to consider that acute sampling of body fluids from an animal (“grab and stab”) involves disturbance and stress responses, including shifts in the acid-base status, due to changes in metabolic rate, muscular contraction, release of stress hormones etc. It is recommended to implant a permanent optode or a catheter, which is used to withdraw blood after adequate recovery. This is especially important in the more alert fishes, cephalopods and decapod crustaceans. If the “grab and stab” approach cannot be avoided, some species should be anaesthetised prior to sampling, using an excessive dose of anaesthetic. The sampling procedure itself, for example through puncturing, needs to be as short and as gentle as possible (for fishes, see for example Welker *et al.*, 2007). The results of such procedures must be interpreted with caution and, if possible, cross-calibrated with analyses in cannulated specimens. Interpretation should be restricted to relative changes. In general, sampling for blood gas analyses should exclude contamination with air bubbles by use of a gas tight syringe and of cannulas filled with Ringer solution. For small animals, for example small invertebrates or larvae, one can use a glass capillary pulled to a small tip (by use of an electrode puller or by hand above a flame). After puncturing the animal body surface, blood or haemolymph is sucked into the glass by capillary forces.

In bivalves, samples of haemolymph have been collected by pericardiac puncture (Fyhn & Costlow, 1975) or from the posterior adductor muscle sinus (e.g. Booth *et al.*, 1984). Samples have been withdrawn from the coelomic cavity of sipunculids after cannulation (Pörtner *et al.*, 1998) or from echinoderms by a “grab and stab” approach (e.g. Spicer *et al.*, 1988). After, or in parallel to rapid analysis for extracellular acid-base parameters, tissues are excised, blotted dry, freeze-clamped and kept under liquid nitrogen until used for the determination of pH_i and buffering capacity (e.g. Michaelidis *et al.*, 2005). For acute blood and tissue sampling in fishes, a concentrated solution of buffered anaesthetic (Tricaine methanesulfonate, MS-222, buffered by the addition of sodium bicarbonate) is slowly added to the aquarium to achieve a species-specific final concentration of, for example, 0.15 g l⁻¹. Within 2 to 3 min, the fish loses balance and can be removed from the water without struggling. The second best approach after cannulation is to withdraw blood from the caudal vein into a heparinised syringe for analysis of extracellular pH (pH_e), P_{CO₂}, [Hb], haematocrit, lactate levels etc. The fish is then killed and tissues (e.g. heart and skeletal muscle) are excised and frozen immediately in liquid nitrogen for later analysis of intracellular pH. Sampling can be completed within 2 to 3 min after the fish has been removed from the water.

Blood and haemolymph collected in gas tight syringes may clot on the surfaces of syringes, electrodes and optode tips. Heparinisation of these surfaces often solves this problem. Since heparin influences the bicarbonate level and arterial CO₂ tensions (P_aCO₂) one should make sure that no liquid heparin is left after flushing (Madiedo *et al.*, 1982). Extracellular acid-base parameters are determined in blood plasma or equivalent. For C_{CO₂} analysis and associated acid treatment this requires the removal of cellular components by centrifugation. This is not usually required for blood gas or pH analyses.

Interstitial pH

Most attention has focused on the properties of intracellular and extracellular bulk fluids when acid-base regulation of an animal is discussed. However, interstitial fluid is the one in contact with the cell membrane and mediates all extracellular signal transfer to the cell. There is no direct method available to investigate the acid-base parameters in the interstitial fluid or on the cellular surface *in vivo*. However, it is important to note that a P_{CO_2} gradient may prevail between the intra- and extracellular fluids which is likely to cause a lower interstitial pH than plasma pH, owing to minimal non-bicarbonate buffering in the interstitial fluid (Pörtner *et al.*, 1991b; Pörtner, 1993). The presence of a P_{CO_2} gradient would explain why pH values are lower on the cell surface than in the surrounding medium or blood and why a pH gradient may prevail from the cell surface to the venous blood or ambient medium (De Hemptinne & Huguenin, 1984). The resulting pH gradient would be larger with rapid CO_2 hydration as expected from the action of extracellular, membrane-bound carbonic anhydrase (e.g. Henry *et al.*, 1997).

The steady state P_{CO_2} gradient between intra- and extracellular space under resting conditions leads to interstitial pH values between 0.1 and 0.15 units lower than in the venous plasma. Some studies have revealed that changes in intracellular and extracellular P_{CO_2} may differ, especially during exercise when intracellular P_{CO_2} surges in poorly perfused tissues such as white muscle. Larger P_{CO_2} gradients between intra- and extracellular space are likely to develop with increased metabolic rate as during exercise (Pörtner *et al.*, 1991a; Boutilier *et al.*, 1993). In poorly perfused white muscle this trend is exacerbated by glycolytic acidification and titration of bicarbonate stores thus leading to even higher intracellular P_{CO_2} levels, steeper P_{CO_2} gradients and lower values of interstitial pH. These considerations emphasise the importance to compile P_{CO_2} estimates in various body compartments in order to gain a more complete picture of acid-base status, especially during metabolic transition phases or during exercise, both of which involve non steady-state conditions.

Intracellular space

Isolated cells and organs

Microelectrode, fluorescent probes and, to some extent, ^{31}P -NMR are most suitable for cellular and subcellular investigations of acid-base parameters in isolated organs and cells (see Schwiening, 1999; Kinsey & Moerland, 1999). At higher levels of complexity, in isolated tissues or transparent animals, fluorescent probes may still be used, as well as ^{31}P -NMR and the homogenate technique (see above). In larger specimens, microelectrode and fluorescent probes are usually no longer applicable, while ^{31}P -NMR and the homogenate techniques are more appropriate.

Whole animals

The first reliable technique to be used in whole animals was the measurement of the pH-dependent distribution of weak acids and bases, in particular the weak acid dimethyl-oxazolidine-dione (DMO), between the intra- and extracellular spaces (Waddell & Butler, 1959; for a review see Roos & Boron (1981)). In brief, DMO is infused in the animal via an indwelling catheter and pH_i is calculated from the DMO distribution and the extracellular pH measured by an electrode (Figure 9.9). The use of radiolabelled DMO makes it possible to determine pH_i invasively in not just one, but various tissues collected from the same individual animal. However, the measurement of rapid pH_i changes, for instance during muscle activity, is limited by the diffusivity of DMO. Further disadvantages arise from the fact that pH_i can only be estimated mathematically from extracellular pH, water content of the tissue, concentrations of radiolabelled inulin and DMO in the tissue and plasma to evaluate the intra- and extracellular DMO concentrations. Each of the required measurements has its own inherent errors, which leads to a relatively high variability in the pH_i values calculated (see above). Therefore, this technique has largely been abandoned. More recently, intracellular pH has been investigated in isolated tissues and whole animals using ^{31}P -NMR (see above) and the homogenate technique (Pörtner *et al.*, 1990). ^{31}P -NMR requires an *in vivo* analysis in the immobilised animal unless the animal exercises in a stable position within the magnet and the spectra are recorded by gating the system (Bock *et al.*, 2008). Prior to the advent of the

homogenate technique the only way to determine intracellular pH during muscular activity of the unrestrained animal was by calculation through pH/bicarbonate analysis from tissue metabolic changes, also considering the exchange of acid-base equivalents between the intra- and extracellular space (Pörtner, 1987a, b).

Cellular compartmentalisation

The pH values determined using homogenates in tissues poor in mitochondria are in good agreement with the mean pH values obtained with DMO (cf. Pörtner *et al.*, 1990) and ³¹P-NMR (e.g. Zange *et al.*, 1990). In cells containing a large number of mitochondria, the pH values obtained with these techniques differ depending on the abundance of mitochondria and on the pH gradient maintained between these organelles and the cytoplasm (the contribution of other organelles appears to be less relevant). The contribution of cellular compartments to the average intracellular (homogenate) pH follows their percent contribution to cellular buffering and their relative volume. For reference, mixing two identical volumes of the same buffer values would yield the arithmetic mean of the two pH values. However, the buffer mixtures differ between the two compartments. CO₂ distribution follows weak acid distribution characteristics. In mitochondria, pH is higher and, consequently, the total CO₂ concentration is higher than in the cytosol. CO₂ partial pressures being equal in cytosol (c) and mitochondrial matrix (m), a pH gradient of 1 between the two compartments causes matrix bicarbonate and, accordingly, Cco₂ levels to be approximately 10-fold higher than those in the cytosol (Pörtner *et al.*, 1990, 1991a, b, cf. Figure 9.9):

$$\frac{[\text{HCO}_3^-]_m}{[\text{HCO}_3^-]_c} = 10^{\Delta\text{pH}} \quad (9.9)$$

During the pH measurement in the homogenate, all buffers (including total CO₂ which comprises the CO₂/bicarbonate buffers) are mixed in a closed system with no exchange of CO₂ between the homogenate and the air. This reduces the influence of the CO₂/bicarbonate buffer on homogenate pH. Furthermore, the CO₂/bicarbonate buffer value is pH-dependent and rather low at high mitochondrial pH. This leads to homogenate derived pH_i values closer to cytosolic pH.

In addition, the comparison of the mean cellular pH obtained by various techniques suggests that mitochondria display non-bicarbonate buffer values lower than the cytosol and do not exert a large influence on mean cellular pH. The concentration and relative contribution of non-bicarbonate buffer substances may thus be different between mitochondrial and cytosolic compartments. Cytosolic actomyosin comprises the major protein fraction in muscle tissue and was found to be 2 to 3 times more important in cellular buffering than soluble protein in trout (Abe *et al.*, 1985). Histidine related compounds such as carnosine and anserine (which are predominantly found in white muscle; Abe *et al.*, 1985) may also prevail in the cytosol. Inorganic phosphate levels are similar or lower in mitochondria than in the cytosol (Soboll & Bünger, 1981). Phosphate is believed to be bound to Ca²⁺ in the mitochondrial matrix and would, therefore, be inefficient in mitochondrial buffering.

As a corollary, differences prevail between techniques in their ability to weight compartmental parameters in the determination of mean intracellular pH. Such parameters are volumes, buffer values and pH values (homogenate technique) or volumes and pH differences only (DMO technique). These approaches therefore lead to different pH_i values when mitochondrial density is high. The homogenate technique provides an estimate of mean intracellular pH emphasising cytosolic pH, whereas the DMO distribution even overestimates mean pH_i largely due to the distribution characteristics of weak acids. With regards to the ³¹P-MRS technique, the localisation of cellular pH is not satisfactorily explained, but this method is also assumed to reflect cytosolic pH (Gadian *et al.*, 1982).

The fact that the various methods yield different mean values of pH_i leads to the question, which is the recommended approach to determine mean intracellular Pco₂ in mitochondria-rich cells? Since the concentrations of Cco₂ in the cytosol and the mitochondria are highly different and determined by the characteristics of weak acid distribution (see above), a mean cellular pH value as expected from the analysis of weak acid distribution is required (see above). pH_i values determined by the DMO technique in individual samples are usually not suitable for this process owing to their large inherent inaccuracy. At present, model considerations of the general difference between homogenate and weak acid derived mean pH_i values are useful to come to reasonable estimates of mean intracellular Pco₂ values in mitochondria-rich tissues.

Quantitative aspects

How do we know whether acid-base variables in organismal compartments and in ambient water have been correctly determined? Cross-calibration using various methods is a suitable way of checking consistency. Furthermore, multi-compartmental assessments of proton production by metabolism or during CO₂ exposures provide a quantitative background of acid-base disturbances (e.g. Pörtner, 1987a, b; Pörtner *et al.*, 1998).

9.5 Overall suggestions for improvements

Several methods are available to study the relationships between acid-base and metabolic regulation and assess the role of acid-base parameters in modulating metabolic rate, energetic parameters and functional capacity under ocean acidification. This includes a comprehensive analysis of acid-base parameters such as intra- and extracellular (as well as interstitial) pH, bicarbonate and Pco₂ levels taking into account the buffering characteristics of each compartment. Specific patterns of acid-base regulation observed in organisms from various phyla need to be considered building on the hypothesis that the molecular mechanisms of acid-base regulation follow unifying principles across phyla.

The study of acid-base physiology has had its heyday in the 1980s and 1990s. Comparative studies were performed using methods originally developed in medical science. The automation of these techniques for use with human blood disconnected the fields, leaving environmental physiology with equipment which is currently available only second or third hand, if at all. New methods are presently developed. They should replace previous techniques and reach similar standards (e.g. optode systems for pH and Pco₂). Further miniaturisation of methods for accurate pH measurements in small sample volumes and body compartments would enable to investigate acid-base equilibria in compartments such as those close to calcification sites. Overall, the successful application of the techniques discussed in the present chapter should build on mechanistic hypotheses and look at acid-base parameters as mediators of physiological effects, which can then be upscaled to ecosystem level (Pörtner & Farrell, 2008).

Epithelia: gill, capillary (gill and tissue)					
Water	Blood plasma	Tissue / Cell			
		Membranes: cell, compartments			
		IF (cell surface)	Cytosol	Mitochondria	
Pco ₂ (Torr) 0.3	1.6	< 3.4	~ 3.4	~ 3.4	
pH _{NBS} 8.1	7.9	> 7.7	> 7.4	<	~ 8.0
HCO ₃ ⁻ 2.3	6.0	> 6.0	> 2.5	<	~20
β _{NB} <1.0	e.g. 5	> 1.0	< e.g. 47	>	e.g. 19

Figure 9.9 Differences in physicochemical variables between seawater, extracellular fluids and cellular compartments (IF: interstitial fluid, β_{NB}: non-bicarbonate buffer value, modified after Pörtner & Sartoris, 1999).

Standardised pH buffers with ionic strengths adjusted to levels similar to those of various body fluids would be ideal for improved accuracy. Standard buffers prepared for analyses in seawater should be suitable to the extracellular fluids of most marine invertebrates (seawater buffers, Dickson *et al.*, 2007; chapter 1 of this guide). If standardised solutions are not commercially available, protocols for buffer preparation must be developed.

In general, the disturbances of the acid-base status caused by ocean acidification can be considered small from the point of view of more traditional physiological analyses, which focus on the identification of contributing mechanisms. They nonetheless become effective on long time scales. Online techniques like NMR appear best suited to monitor acid-base parameters long-term and to minimise disturbance to the living organism. However, it remains to be established which “online” techniques (NMR and fluorescent dyes) can be developed to provide the most suitable assay for the long-term determination of acid-base disturbances under ocean acidification scenarios.

9.6 Data reporting

- **Information required to fully describe the experimental procedure:** exposure regime, duration of exposure, water physicochemistry values (levels of e.g. pH, bicarbonate, carbonate, calcium) on physiologically relevant scales.
- **Information required to fully describe the sampling methods:** for example animal acclimation and treatment, sampling procedure for tissues, dye, wavelengths of excitation and emission, time resolution and spatial resolution (whole tissue layer, whole cell, cellular compartment).
- **Metadata:** tissue and cell type, parameters investigated, experimental tools (buffer systems, calibration procedures, ion gradients, pharmacological tools (specific transport inhibitors, inhibitors of carbonic anhydrase)).
- **Raw data recorded to characterise an experimental system (no reporting to community necessary):** for example fluorescence intensities vs. wavelength in a region of interest (AU, arbitrary units) and variability between replicates.
- **Data:** for example ratio as a signal which is linearly correlated to pH in a given range (AU), pH, H⁺ flux (nmol H⁺/time × membrane area), time constants for pH recovery due to systemic or cellular mechanisms, relative percent change in paired experiments.
- Rate of pH change (τ) during the pH disturbance or recovery phases.
- Comprehensive set of acid-base variables during the quantitative treatment of the acid-base status.

9.7 References

- Abe H., Dobson G. P., Hoeger U. & Parkhouse W. S., 1985. Role of histidine-related compounds to intracellular buffering in fish skeletal muscle. *American Journal of Physiology* 249:R449-R454.
- Atkinson D. E. & Bourke E., 1995. pH homeostasis in terrestrial vertebrates; ammonium ion as a proton source. *Advances in Comparative and Environmental Physiology* 22:3-26.
- Bailey D. M., Peck L. S., Bock C. & Pörtner H.-O., 2003. High-energy phosphate metabolism during exercise and recovery in temperate and Antarctic scallops: an in vivo ³¹P-NMR study. *Physiological and Biochemical Zoology* 76:622-633.
- Berry L. S., 2001. *Calcification, photosynthesis and calcium uptake in coccolithophores*. PhD Thesis, University of Wales, 267 pp.
- Bickmeyer U., Grube A., Klings K. W. & Köck M., 2008. Ageladine A, a pyrrole-imidazole alkaloid from marine sponges, is a pH sensitive membrane permeable dye. *Biochemical and Biophysical Research Communications* 373:419-422.
- Biemesderfer D., J P., Abu-Alfa A., Exner M., Reilly R., Igarashi P. & Aronson P. S., 1993. NHE3: a Na⁺/H⁺ exchanger isoform of renal brush border. *American Journal of Physiology* 265:F736-F742.

- Bleich M., Köttgen M., Schlatter E. & Greger R., 1995. Effect of $\text{NH}_4^+/\text{NH}_3$ on cytosolic pH and the K^+ channels of freshly isolated cells from the thick ascending limb of Henle's loop. *Pflügers Archiv - European Journal of Physiology* 429:345-354.
- Bleich M., Warth R., Thiele I. & Greger R., 1998. pH-regulatory mechanisms in in vitro perfused rectal gland tubules of *Squalus acanthias*. *Pflügers Archiv - European Journal of Physiology* 436:248-254.
- Bock C., Lurman G. J., Wittig R. M., Webber D. M. & Pörtner H.-O., 2008. Muscle bioenergetics of speeding fish: In vivo ^{31}P -NMR studies in a 4.7 T MR scanner with an integrated swim tunnel. *Concepts in Magnetic Resonance Part B (Magnetic Resonance Engineering)* 33B:62-73.
- Bock C., Sartoris F. J. & Pörtner H.-O., 2002. In vivo MR spectroscopy and MR imaging on non-anaesthetized marine fish: techniques and first results. *Magnetic Resonance Imaging* 20:165-172.
- Booth C. E., McDonald D. G. & Walsh P. J., 1984. Acid-base balance in the sea mussel, *Mytilus edulis*. 1. Effects of hypoxia and air exposure on hemolymph acid-base status. *Marine Biology Letters* 5:347-358.
- Bothwell J. H. F., Brownlee C., Hetherington A. M., Ng C. K. Y., Wheeler G. L. & McAinsh M. R., 2006. Biolistic delivery of Ca^{2+} dyes into plant and algal cells. *Plant Journal* 46:327-335.
- Boutilier R. G., Ferguson R. A., Henry R. P. & Tufts B. L., 1993. Exhaustive exercise in the sea lamprey (*Petromyzon marinus*): relationships between anaerobic metabolism and intracellular acid-base balance. *Journal of Experimental Biology* 178:71-88.
- Boutilier R. G., Iwama G. K., Heming T. A. & Randall D. J., 1985. The apparent pK of carbonic acid in rainbow trout blood plasma between 5°C and 15°C. *Respiratory Physiology* 61:237-254.
- Buck R. P., Rondini S., Covington A. K., Baucke F. G. K., Brett C. M. A., Camoes M. F., Milton M. J. T., Mussini T., Naumann R., Pratt K. W., Spitzer P. & Wilson G. S., 2002. Measurement of pH. Definition, standards, and procedures. *Pure and Applied Chemistry* 74:2169-2200.
- Cameron J. N., 1986. *Principle of physiological measurement*. 278 p. Orlando: Academic Press Orlando.
- Cameron J. N., 1989. Acid-base homeostasis: past and present perspectives. *Physiological Zoology* 62:845-865.
- Daniel H. & Kottra G., 2004. The proton oligopeptide cotransporter family SLC15 in physiology and pharmacology. *Pflügers Archiv - European Journal of Physiology* 447:610-618.
- de Hemptinne A. & Huguenin F., 1984. The influence of muscle respiration and glycolysis on surface and intracellular pH in fibres of the rat soleus. *Journal of Physiology* 347:581-592.
- Dickson A. G., Sabine C. L. & Christian J. R. (Eds.), 2007. Guide to best practices for ocean CO_2 measurements. *PICES Special Publication* 3:1-191.
- Dixon G. K., Brownlee C. & Merrett M. J., 1989. Measurement of intracellular pH in the coccolithophore *Emiliania huxleyi* using 2',7'-bis-(2-carboxyethyl)-5-(and-6)carboxyfluorescein acetoxymethyl ester and digital imaging microscopy. *Planta* 178:443-449.
- Eisner D. A., Kenning N. A., O'Neill S. C., Pocock G., Richards C. D. & Valdeolmillos M., 1989. A novel method for absolute calibration of intracellular pH indicators. *Pflügers Archiv - European Journal of Physiology* 413:553-558.
- Farinas J. & Verkman A. S., 1999. Receptor-mediated targeting of fluorescent probes in living cells. *Journal of Biological Chemistry* 274:7603-7606.
- Ferguson R. A., Kieffer J. D. & Tufts B. L., 1993. The effects of body size on the acid-base and metabolite status in the white muscle of rainbow trout before and after exhaustive exercise. *Journal of Experimental Biology* 180:195-207.
- Frederich M. & Pörtner H.-O., 2000. Oxygen limitation of thermal tolerance defined by cardiac and ventilatory performance in spider crab, *Maja squinado*. *American Journal of Physiology* 279:R1531-R1538.
- Fujita M., Nakao Y., Matsunaga S., Seiki M., Itoh Y., Yamashita J., van Soest R. W. M. & Fusetani N., 2003. Bioactive marine metabolites, Part 124. Ageladine A: an antiangiogenic matrix metalloproteinase inhibitor from the marine sponge *Agelas nakamurai*. *Journal of the American Chemical Society* 125:15700-15701.
- Fyhn H. J. & Costlow J. D., 1975. Anaerobic sampling of body fluids in bivalve molluscs. *Comparative Biochemistry and Physiology - Part A* 52:265-268.

- Gadian D. G., Radda G. K., Dawson M. J. & Wilkie D. R., 1982. pH_i measurements of cardiac and skeletal muscle using ³¹P-NMR. In: Nuccitelli R. & Deamer D. W. (Eds.), *Intracellular pH: Its measurement, regulation and utilization in cellular functions*, pp. 61-77. New York: Alan R. Liss Inc.
- Garcia-Martin M. L., Martinez G. V., Raghunand N., Sherry A. D., Zhang S. R. & Gillies R. J., 2006. High resolution pH_c imaging of rat glioma using pH-dependent relaxivity. *Magnetic Resonance in Medicine* 55:309-315.
- Gibbon B. C. & Kropf D. L., 1994. Cytosolic pH gradients associated with tip growth. *Science* 263:1419-1421.
- Gillies R. J., Liu Z. & Bhujwala Z., 1994. ³¹P-MRS measurements of extracellular pH of tumors using 3-aminopropylphosphonate. *American Journal of Physiology* 267:C195-C203.
- Gillies R. J., Raghunand N., Garcia-Martin M. L. & Gatenby R. A., 2004. pH imaging. A review of pH measurement methods and applications in cancers. *IEEE Engineering in Medicine and Biology* 23:57-64.
- Gutowska M. & Melzner F., 2009. Abiotic conditions in cephalopod (*Sepia officinalis*) eggs: embryonic development at low pH and high pCO₂. *Marine Biology* 156:515-519.
- Gutowska, M.A., Melzner F., Langenbuch M., Bock C., Claireaux G. & Pörtner H.O.. Acid-base regulatory ability of the cephalopod (*Sepia officinalis*) in response to environmental hypercapnia. *Journal of Comparative Physiology – B* DOI 10.1007/s00360-009-0412-y
- Haber F. & Klemensiewicz Z., 1909. Über elektrische Phasengrenzkräfte. *Zeitschrift für Physikalische Chemie* 64:385- 391.
- Hardewig I., Pörtner H.-O. & Grieshaber M. K., 1994. Interactions of anaerobic propionate formation and acid-base status in *Arenicola marina*: an analysis of propionyl-CoA-carboxylase. *Physiological Zoology* 67:892-909.
- Haugland R. P., Spence M. T. Z., Johnson I. D. & Basey A., 2005. *The handbook: a guide to fluorescent probes and labeling technologies*. 1126 p. Eugene, Oregon: Molecular Probes.
- Heisler N., 1975. Intracellular pH of isolated rat diaphragm muscle with metabolic and respiratory changes of extracellular pH. *Respiratory Physiology* 23:243-255.
- Heisler N., 1989. Parameters and methods in acid-base physiology. In: Bridges C. R. & Butler P. J. (Eds.), *Techniques in comparative respiratory physiology*, pp. 305-332. Cambridge: Cambridge University Press.
- Heisler N. & Neumann P., 1980. The role of physicochemical buffering and of bicarbonate transfer processes in intracellular pH regulation in response to changes of temperature in the larger spotted dogfish (*Scyliorhinus stellaris*). *Journal of Experimental Biology* 85:99-110.
- Heisler N. & Piiper J., 1971. The buffer value of rat diaphragm muscle tissue determined by PCO₂ equilibration of homogenates. *Respiratory Physiology* 12:169-178.
- Heisler N., 1984. Acid–base regulation in fishes. In: Hoar W. S. & Randall D. J. (Eds.), *Fish Physiology*, vol. XA, pp. 315–401. New York: Academic Press.
- Heisler N., 1986. Buffering and transmembrane ion transfer processes. In: Heisler N. (Ed.), *Acid–base regulation in animals*, pp. 3–47. Amsterdam: Elsevier Biomedical Press.
- Henry R. P., Wang Y. X. & Wood C. M., 1997. Carbonic anhydrase facilitates CO₂ and NH₃ transport across the sarcolemma of trout white muscle. *American Journal of Physiology* 272:R1754-R1761.
- Hochachka P. W. & Mommsen T. P., 1983. Protons and anaerobiosis. *Science* 219:1391-1397.
- James-Kracke M. R., 1992. Quick and accurate method to convert BCECF fluorescence to pH_i calibration in three different types of cell preparations. *Journal of Cellular Physiology* 151:596-603.
- Kinsey S. T. & Moreland T., 1999. The use of nuclear magnetic resonance for examining pH in living systems. In: Taylor E. W., Egington S. & Raven J. A. (Eds.), *Regulation of tissue pH in plants and animals. SEB Seminar Series*, pp. 45-67. Cambridge: Cambridge University Press.
- Kneen M., Farinas J., Li Y. X. & Verkman A. S., 1998. Green fluorescent protein as a noninvasive intracellular pH indicator. *Biophysical Journal* 74:1591-1599.
- Kosch U., Klimant I., Werner T. & Wolfbeis O. S., 1998. Strategies to design pH optodes with luminescence decay times in the sensorsecond time regime. *Analytical Chemistry* 362:73-78.

- Kost G. J., 1990. pH standardization for phosphorus-31 magnetic resonance heart spectroscopy at different temperatures. *Magnetic Resonance in Medicine* 14:496-506.
- Kotyk A. & Slavik J., 1989. *Intracellular pH and its measurement*. 192 p. Boca Raton: CRC Press.
- Kratz L., 1950. *Die Glaselektrode und ihre Anwendungen*. 380 p. Frankfurt: Verlag Dr. Dietrich Steinkopff.
- Krause U. & Wegener G., 1996. Exercise and recovery in frog muscle: metabolism of PCr, adenine nucleotides, and related compounds. *American Journal of Physiology* 270:R811-R820.
- Lannig G., Bock C., Sartoris F. J. & Pörtner H.-O., 2004. Oxygen limitation of thermal tolerance in cod, *Gadus morhua* L., studied by magnetic resonance imaging and on-line venous oxygen monitoring. *American Journal of Physiology* 287:R902-R910.
- Lenfant C. & Aucott C., 1966. Measurement of blood gases by gas chromatography. *Respiratory Physiology* 1:398-407.
- Liebsch G., Klimant I., Krause C. & Wolfbeis O. S., 2001. Fluorescent imaging of pH with optical sensors using time domain dual lifetime referencing. *Analytical Chemistry* 73:4354-4363.
- Madden A., Leach M. O., Sharp J.C., Collins D. J., Easton D., 1991. A quantitative analysis of the accuracy of in vivo pH measurements with ³¹P NMR spectroscopy: assessment of pH measurement methodology. *NMR in Biomedicine* 4: 1-11.
- Madiedo G., Sciacca R., Hause L. & Sasse E., 1982. Use of syringes containing dry (lyophilized) heparin in sampling blood for pH measurement and blood-gas analysis. *Clinical Chemistry* 28:1727-1729.
- Meketa M. L. & Weinreb S. M., 2006. Total synthesis of ageladine A, an angiogenesis inhibitor from the marine sponge *Agelas nakamurai*. *Organic Letters* 8:1443-1446.
- Meketa M. L., Weinreb S. M., Nakao Y. & Fusetani N., 2007. Application of a 6π-1-azatriene electrocyclization strategy to the total synthesis of the marine sponge metabolite ageladine A and biological evaluation of synthetic analogues. *Journal of Organic Chemistry* 72:4892-4899.
- Meketa M. L. & Weinreb S. M., 2007. A convergent total synthesis of the marine sponge alkaloid ageladine A via a strategic 6π-2-azatriene electrocyclization. *Tetrahedron* 63:9112-9119.
- Melzner F., 2005. *Systemic investigations on the physiology of temperature tolerance in the common cuttlefish Sepia officinalis*. PhD Thesis, University of Bremen, 234 p.
- Melzner F., Bock C. & Pörtner H.-O., 2006. Critical temperatures in the cephalopod *Sepia officinalis* investigated using in vivo ³¹P-NMR spectroscopy. *Journal of Experimental Biology* 209:891-906.
- Melzner F., Bock C. & Pörtner H.-O., 2006. Temperature-dependent oxygen extraction from the ventilatory current and the costs of ventilation in the cephalopod *Sepia officinalis*. *Journal of Comparative Physiology B* 176:607-621.
- Metzger R., Sartoris F. J., Langenbuch M. & Pörtner H.-O., 2007. Influence of elevated CO₂ concentrations on thermal tolerance of the edible crab *Cancer pagurus*. *Journal of Thermal Biology* 32:144-151.
- Michaelidis B., Ouzounis C., Paleras A. & Pörtner H.-O., 2005. Effects of long-term moderate hypercapnia on acid-base balance and growth rate in marine mussels (*Mytilus galloprovincialis*). *Marine Ecology Progress Series* 293:109-118.
- Michard E., Dias P. & Feijo J. A., 2008. Tobacco pollen tubes as cellular models for ion dynamics: improved spatial and temporal resolution of extracellular flux and free cytosolic concentration of calcium and protons using pHluorin and YC3.1 CaMeleon. *Sexual Plant Reproduction* 21:169-181.
- Moon R. B. & Richards J. H., 1973. Determination of intracellular pH by ³¹P Magnetic Resonance. *Journal of Biological Chemistry* 248:7276-7278.
- Musgrove E., Rugg C. & Hedley D., 1986. Flow cytometric measurement of cytoplasmic pH – a critical evaluation of available fluorochromes. *Cytometry* 7:347-355.
- Palmer A. E. & Tsien R. Y., 2006. Measuring calcium signaling using genetically targetable fluorescent indicators. *Nature Protocols* 1:1057-1065.
- Poenie M., 1990. Alteration of fura-2 fluorescence by viscosity – a simple correction. *Cell Calcium* 11:85.
- Pörtner H.-O., 1987. Anaerobic metabolism and changes in acid-base status: quantitative interrelationships and pH regulation in the marine worm *Sipunculus nudus*. *Journal of Experimental Biology* 131:89-105.

Part 3: Measurements of CO₂ -sensitive processes

- Pörtner H.-O., 1987. Contributions of anaerobic metabolism to pH regulation in animal tissues: theory. *Journal of Experimental Biology* 131:69-87.
- Pörtner H.-O., 1989. The importance of metabolism in acid base regulation and acid base methodology. *Canadian Journal of Zoology* 67:3005-3017.
- Pörtner H.-O., 1990. An analysis of the effects of pH on oxygen binding by squid (*Illex illecebrosus*, *Loligo pealei*) haemocyanin. *Journal of Experimental Biology* 150:407-424.
- Pörtner H.-O., 1990. Determination of intracellular buffer values after metabolic inhibition by fluoride and nitrilotriacetic acid. *Respiratory Physiology* 81:275-288.
- Pörtner H.-O., 1993. Multicompartmental analyses of acid-base and metabolic homeostasis during anaerobiosis: invertebrate and lower vertebrate examples. In: Hochachka P. W., Lutz P. L., Sick T., Rosenthal M. & van den Thillart G. (Eds.), *Surviving hypoxia: mechanisms of control and adaptation*, pp. 139-156. Boca Raton: CRC Press.
- Pörtner H.-O., Bock C. & Reipschläger A., 2000. Modulation of the cost of pH_i regulation during metabolic depression: A ³¹P-NMR study in invertebrate (*Sipunculus nudus*) isolated muscle. *Journal of Experimental Biology* 203:2417-2428.
- Pörtner H.-O., Boutilier R. G., Tang Y. & Toews D. P., 1990. Determination of intracellular pH and PCO₂ after metabolic inhibition by fluoride and nitrilotriacetic acid. *Respiratory Physiology* 81:255-274.
- Pörtner H.-O. & Farrell A. P., 2008. ECOLOGY: Physiology and climate change. *Science* 322:690-692.
- Pörtner H.-O., Finke E. & Lee P. G., 1996. Metabolic and energy correlates of intracellular pH in progressive fatigue of squid (*L. brevis*) mantle muscle. *American Journal of Physiology* 271:R1403-R1414.
- Pörtner H.-O., Hardewig I., Sartoris F. J. & van Dijk P., 1998. Energetic aspects of cold adaptation: critical temperatures in metabolic, ionic and acid-base regulation? In: Pörtner H. O. & Playle R. (Eds.), *Cold ocean physiology*, pp. 88-120. Cambridge: Cambridge University Press.
- Pörtner H.-O., Langenbuch M. & Michaelidis B., 2005. Synergistic effects of temperature extremes, hypoxia, and increases in CO₂ on marine animals: from Earth history to global change. *Journal of Geophysical Research- Oceans* 110, C09S10. doi:10.1029/2004JC002561.
- Pörtner H.-O., MacLachy L. M. & Toews D. P., 1991. Acid-base regulation in the toad *Bufo marinus* during environmental hypoxia. *Respiratory Physiology* 85:217-230.
- Pörtner H.-O., Reipschläger A. & Heisler N., 1998. Acid-base regulation, metabolism and energetics in *Sipunculus nudus* as a function of ambient carbon dioxide level. *Journal of Experimental Biology* 201:43-55.
- Pörtner H.-O. & Sartoris F. J., 1999. Invasive studies of intracellular acid-base parameters: quantitative analyses during environmental and functional stress. In: Taylor E. W., Egington S. & Raven J. A. (Eds.), *Regulation of tissue pH in plants and animals. SEB Seminar Series*, pp. 68-98. Cambridge: Cambridge University Press.
- Pörtner H.-O., Webber D. M., Boutilier R. G. & O'Dor R. K., 1991. Acid-base regulation in exercising squid (*Illex illecebrosus*, *Loligo pealei*). *American Journal of Physiology* 261:R239-R246.
- Pörtner H.-O., 1995. pH homeostasis in terrestrial vertebrates: a comparison of traditional and new concepts. *Advances in Comparative and Environmental Physiology* 22:51-62.
- Prakash E. S., Robergs R. A., Miller B. F., Gladden L. B., Jones N., Stringer W. W., Wasserman K., Moll W., Gros G., Rowlands D. S., Sahlin K. & Beneke R., 2008. Comments on point: counterpoint lactic acid is/ is not the only physicochemical contributor to the acidosis of exercise. *Journal of Applied Physiology* 105:363-367.
- Reeves R. B., 1972. An imidazole alaphstat hypothesis for vertebrate acid-base regulation: Tissue carbon dioxide content and body temperature in bullfrogs. *Respiratory Physiology* 14:219-236.
- Reeves R. B., 1985. Alaphstat regulation of intracellular acid-base state? In: Gilles R. (Ed.), *Circulation, respiration, and metabolism*, pp. 414-423. Berlin: Springer-Verlag.
- Reipschläger A. & Pörtner H.-O., 1996. Metabolic depression during environmental stress: The role of extracellular versus intracellular pH in *Sipunculus nudus*. *Journal of Experimental Biology* 199:1801-1807.

- Rink T. J., Tsien R. Y. & Pozzan T., 1982. Cytoplasmic pH and free Mg^{2+} in lymphocytes. *Journal of Cell Biology* 95:189-196.
- Robergs R. A., Ghiasvand F. & Parker D., 2004. Biochemistry of exercise-induced metabolic acidosis. *American Journal of Physiology* 287:R502-R516.
- Roberts J. K. M., Wade-Jardetzky N. & Jardetzky O., 1981. Intracellular pH measurements by ^{31}P nuclear magnetic resonance. Influence of factors other than pH on ^{31}P chemical shifts. *Biochemistry* 20:5389-5394.
- Roos A. & Boron W. F., 1981. Intracellular pH. *Physiological Reviews* 61:296-434.
- Sankaranarayanan S., De Angelis D., Rothman J. E. & Ryan T. A., 2000. The use of pHluorins for optical measurements of presynaptic activity. *Biophysical Journal* 79:2199-2208.
- Sartoris F. J., Bock C., Serendero I., Lannig G. & Pörtner H.-O., 2003. Temperature-dependent changes in energy metabolism, intracellular pH and blood oxygen tension in the Atlantic cod, *Gadus morhua*. *Journal of Fish Biology* 62:1239-1253.
- Schwiening C. J., 1999. Measurement of intracellular pH: a comparison between ion-sensitive electrodes and fluorescent dyes. In: Taylor E. W., Egington S. & Raven J. A. (Eds.), *Regulation of tissue pH in plants and animals. SEB Seminar Series*, pp. 1-17. Cambridge: Cambridge University Press.
- Shengule S. R. & Karuso P., 2006. Concise total synthesis of the marine natural product ageladine A. *Organic Letters* 8:4083-4084.
- Siggaard-Andersen O., 1974. *The acid-base status of the blood*. 229 p. Baltimore: William & Wilkins.
- Soboll S. & Bünger R., 1981. Compartmentation of adenine nucleotides in the isolated working guinea pig heart stimulated by noradrenaline. *Hoppe Seylers Z Physiol Chem* 362:125-132.
- Somero G. N., 1986. Protons, osmolytes and the fitness of the internal milieu for protein function. *American Journal of Physiology* 251:R197-R213.
- Spicer J. I., Taylor A. C. & Hill A. D., 1988. Acid-base status in the sea-urchins *Psammechinus miliaris* and *Echinus esculentus* (Echinodermata, Echinoidea) during emersion. *Marine Biology* 99:527-534.
- Tang Y. & Boutilier R. G., 1991. White muscle intracellular acid-base and lactate status following exhaustive exercise: a comparison between freshwater- and seawater-adapted rainbow trout. *Journal of Experimental Biology* 156:153-171.
- Thatje, S., Calcagno, J. A., Lovrich, G. A., Sartoris, F. J., Anger, K. (2003). Extended hatching periods in the subantarctic lithodid crabs *Lithodes santolla* and *Paralomis granulosa* (Crustacea: Decapoda: Lithodidae), *Helgoland Marine Research*, 57:110-113.
- Thomas J. A., Buchsbaum R. N., Zimniak A. & Racker E., 1979. Intracellular pH measurements in Ehrlich ascites tumor cells utilizing spectroscopic probes generated in situ. *Biochemistry* 18:2210-2218.
- Trapp S., Luckermann M., Brooks P. A. & Ballanyi K., 1996. Acidosis of rat dorsal vagal neurons in situ during spontaneous and evoked activity. *Journal of Physiology* 496:695-710.
- van Sluis R., Bhujwala Z. M., Raghunand N., Ballesteros P., Alvarez J., Cerdán S., Galons J. P. & Gillies R. J., 1999. In vivo imaging of extracellular pH using 1H -MRSI. *Magnetic Resonance in Medicine* 41:743-750.
- Waddell W. J. & Butler T. C., 1959. Calculation of intracellular pH from the distribution of 5,5-dimethyl-2,4-oxazolidine-dione (DMO). Application to skeletal muscle of the dog. *Journal of Clinical Investigation* 38:720-729.
- Walsh P. J. & Milligan C. L., 1989. Coordination of metabolism and intracellular acid-base status: ionic regulation and metabolic consequences. *Canadian Journal of Zoology* 67:2994-3004.
- Welker T. L., Lim C. E., Aksoy M. & Klesius P. H., 2007. Effect of buffered and unbuffered tricaine methanesulfonate (ms-222) at different concentrations on the stress responses of channel catfish (*Ictalurus punctatus* Rafinesque). *Journal of Applied Aquaculture* 19:1-18.
- Wiseman R. W. & Ellington W. R., 1989. Intracellular buffering capacity in molluscan muscle: superfused muscle vs. homogenates. *Physiology and Zoology* 62:541-558.
- Wolfbeis O. S. (Ed.), 1991. *Fiber Optic Chemical Sensors and Biosensors*, Vol. 1 & 2, 359 p. Boca Raton: CRC Press.

- Wollenberger A., Ristau O. & Schoffa G., 1960. Eine einfache Technik der extrem schnellen Abkühlung größerer Gewebestücke. *Pflügers Archiv - European Journal of Physiology* 270:399-412.
- Zange J., Pörtner H.-O., Jans A. W. H. & Grieshaber M. K., 1990. The intracellular pH of a molluscan smooth muscle during a contraction catch relaxation cycle as estimated by the distribution of ^{14}C -DMO and by ^{31}P -NMR spectroscopy. *Journal of Experimental Biology* 150:81-93.
- Zeebe R. E. & Wolf-Gladrow D. A., 2001. *CO₂ in seawater: equilibrium, kinetics, isotopes*. 346 p. Amsterdam: Elsevier.
- Zhao J. H., Hogan E. M., Bevensee M. O. & Boron W. F., 1995. Out-of-equilibrium CO₂/HCO₃⁻ solutions and their use in characterizing a new K/HCO₃ cotransporter. *Nature* 374(6523): 636-639.
- Zhou J. Y., Payen J. F., Wilson D. A., Traystman R. J. & van Zijl P. C. M., 2003. Using the amide proton signals of intracellular proteins and peptides to detect pH effects in MRI. *Nature Medicine* 9:1085-1090.